

Transport in the Middle Atmosphere

Theodore G. SHEPHERD

Department of Physics, University of Toronto, Toronto, Canada

(Manuscript received 12 February 2007, in final form 30 April 2007)

Abstract

An overview is provided of the current understanding of transport in the middle atmosphere. Over the past quarter century this subject has evolved from a basic recognition of the Brewer-Dobson circulation to a detailed appreciation of many key features of transport such as the stratospheric surf zone, mixing barriers, and the dynamics of filamentation. Whilst the elegant theoretical framework for middle atmosphere transport that emerged roughly twenty years ago never fulfilled its promise, useful phenomenological models have been developed together with innovative diagnostic methods. These advances were made possible by the advent of plentiful satellite and aircraft observations of long-lived chemical species together with developments in data assimilation and numerical modeling, and have been driven in large measure by the problem of stratospheric ozone depletion. This review is primarily focused on the stratosphere, where both the interest and the knowledge are the greatest, but a few remarks are also made on the mesosphere.

1. Introduction

Transport has long been an important subject within middle atmosphere science, mainly because of the stratospheric ozone layer. Ozone is essential for shielding life on Earth from the harmful effects of ultraviolet radiation, and is also an important greenhouse gas. Yet the spatial distribution of ozone is strongly affected by transport, especially in the lower stratosphere where the photochemical lifetime of ozone is several months, comparable to transport timescales. Indeed the ozone distribution itself was one of the earliest indicators of what is now called the “Brewer-Dobson circulation”.

The problem of stratospheric ozone depletion led to a rapid development of research into stratospheric transport in the late 1980s and through the 1990s, which exploited aircraft and satellite measurements of multiple chemi-

cal species as well as the availability of global data sets of analyzed winds. Transport proved to be important in understanding many aspects of the ozone depletion problem—e.g., the isolation of the Antarctic polar vortex that allows severe depletion to occur—as well as in explaining some of the long-term variations in ozone abundance that cannot be attributed to chemical ozone depletion. During the anticipated recovery of the ozone layer over the next half-century, as ozone-depleting halogens are slowly removed from the stratosphere, changes in transport associated with climate change would affect both the removal rate of the halogens and the future distribution of ozone.

There has been much recent interest in the interface between the troposphere and stratosphere, now generally called the “upper troposphere/lower stratosphere” (UTLS), as a nexus for chemistry-climate coupling. Because of the low temperatures in this region, radiative forcing is especially sensitive to the distribution of greenhouse gases in the UTLS; and for the shorter-lived, non-well-mixed greenhouse gases (ozone and water vapor), these dis-

Corresponding author: Theodore G. Shepherd, Department of Physics, University of Toronto, 60 St. George Street, Toronto, M5S 1A7, Canada.
E-mail: tgs@atmosph.physics.utoronto.ca
© 2007, Meteorological Society of Japan

tributions are sensitive to transport. Furthermore the flux of ozone from the stratosphere to the troposphere affects the tropospheric ozone budget and the oxidizing capacity of the troposphere.

Quite apart from the importance of transport for ozone chemistry and radiative forcing, long-lived tracers also provide a way of inferring properties of middle atmosphere dynamics. Because the middle atmosphere is relatively quiescent (compared with the troposphere) and its overturning timescale slow (about five years), long-lived tracers such as N_2O and CH_4 (with lifetimes of decades) provide useful indicators of circulation and mixing. Even very long-lived tracers such as CO_2 can be useful because of their secular growth with time and their annual cycle in the troposphere. This is fortunate, because dynamical measurements in the middle atmosphere are quite limited. In particular there are no direct measurements of winds apart from those provided by radiosondes, which are limited to below about 30 km and over land, leaving enormous gaps in the tropics, the Southern Hemisphere (SH), and the mid to upper stratosphere.

A major development within atmospheric science that has already begun and will be of increasing importance in the coming decade is the extension of data assimilation systems into the mesosphere (in order to fully resolve the stratosphere), and the inclusion of interactive ozone chemistry (in order to better assimilate radiances). There is also a general movement towards comprehensive environmental modeling including coupled chemistry. This raises the prospect of ongoing chemical-dynamical analyses of the middle atmosphere. However chemical observations may often be sparse or even non-existent, and even the best-observed species (such as ozone) may not be sufficiently well sampled to strongly constrain the assimilating model. Thus, assessing the value of these analyses will require diagnostic tools that properly capture key aspects of middle atmosphere transport and relationships between different species.

For all these reasons, transport in the middle atmosphere is a fascinating subject of contemporary relevance. The purpose of this article is to provide an overview of the subject, with pointers to references where more detailed in-

formation can be obtained. It is aimed at atmospheric scientists but does not presume any previous knowledge of the middle atmosphere. An introduction to some of the basic dynamical concepts and a glossary of technical terms can be found in Shepherd (2003). The article mainly focuses on the stratosphere, although some remarks are made on the mesosphere. However, transport processes associated with the complex dynamics of the mesosphere/lower thermosphere (MLT) region are beyond the scope of this review.

2. The Brewer-Dobson circulation

The stratosphere is primarily distinguished from the troposphere by its stability—as its very name suggests. The troposphere is heated from below and undergoes both convective and baroclinic instability. In contrast the stratosphere is heated radiatively from within and is, for the most part, dynamically stable. In the absence of any other forcing, we could then expect the stratosphere to be close to radiative equilibrium, with a slight time lag because of the finite radiative relaxation time (less than one month). This would be a rather boring (albeit non-trivial) state: zonal flow, in thermal wind balance with radiative equilibrium, and essentially no meridional circulation.

However the stratosphere is forced away from radiative equilibrium, by waves propagating up from the troposphere which transfer angular momentum and energy. The energy transfer is not a significant part of the energy budget, because any heating from energy deposition can be radiated to space. In contrast, any systematic transfer of angular momentum can only be balanced by the Coriolis torque associated with a latitudinal mass flux within the stratosphere. By mass conservation a latitudinal mass flux must induce upwelling and downwelling. Because radiative heating is generally relaxational, it can accommodate these implied vertical circulations. For example, downwelling produces adiabatic warming which induces radiative cooling, allowing the downwelling to persist. A latitudinal return flow can be realized in the planetary boundary layer, because of the relaxational nature of friction. This is the theory of “downward control” (Haynes et al. 1991), which relates steady meridional circulations to imposed torques. Such circulations,

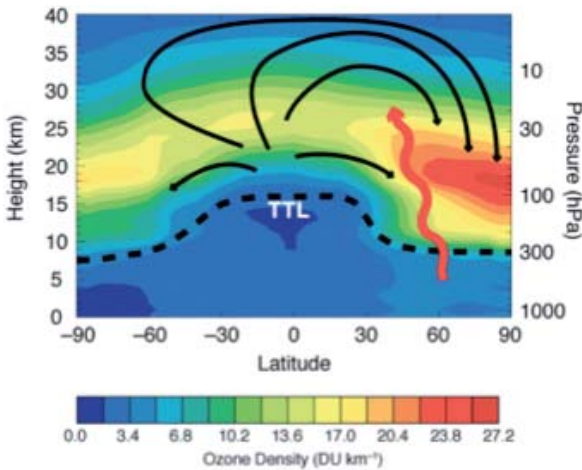


Fig. 1. Meridional cross-section of the atmosphere up to 40 km altitude showing ozone density (color contours in Dobson units (DU) per km) averaged from January to March, from the climatology of Fortuin and Kelder (1998). The dashed line indicates the tropopause, and “TTL” stands for tropical tropopause layer (see Section 6). The black arrows indicate the Brewer-Dobson circulation during NH winter, and the wiggly red arrow represents planetary waves that propagate from the troposphere into the winter stratosphere. Reprinted with permission from Chapter 1 of IPCC/TEAP (2005), copyright Cambridge University Press.

which characterize the middle atmosphere, are mechanically driven and thermally damped, like a refrigerator (e.g., Shepherd 2000). In contrast, the troposphere may be regarded as a heat engine (Barry et al. 2002).

Such wave-driven circulations alter the temperature and, hence, the zonal wind of the stratosphere. Moreover the waves themselves lead to longitudinal variations in the state of the stratosphere. What are the waves that are relevant? In both hemispheres and in all seasons, synoptic-scale Rossby-wave disturbances, mainly associated with baroclinic instability, dissipate in the subtropical lower stratosphere (Held and Hoskins 1985). The applied torque is always negative for dissipating Rossby waves; this is a consequence of their negative intrinsic phase speed, and can be seen in various ways (see e.g., Shepherd 2000; McIntyre

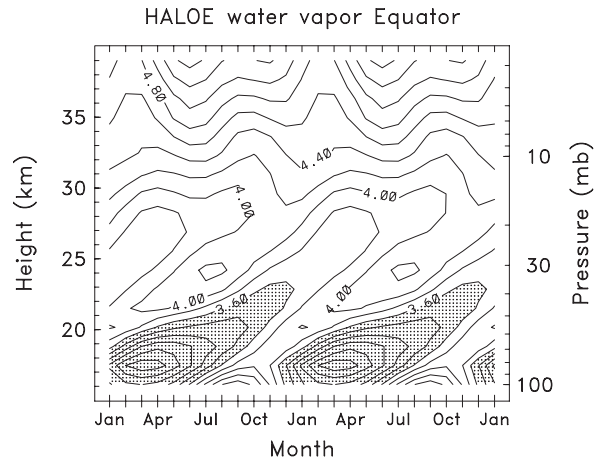


Fig. 2. Time-height cross-section of the annual cycle of water vapor at the equator, in parts per million by volume, from a climatology produced from the HALOE instrument on the UARS satellite. The data set is described in Randel et al. (1998), and two annual cycles are shown for clarity. There is clear evidence of upward propagation of the annual cycle in tropopause dehydration, up to about 30 km. Furthermore the drier part of the cycle evidently propagates faster (above 20 km), as expected since lower temperatures imply stronger upwelling. Figure courtesy of Bill Randel, National Center for Atmospheric Research.

2000). In consequence, synoptic-scale disturbances drive a persistent poleward circulation in both hemispheres of the lower stratosphere.

At higher altitudes, there is a fundamental asymmetry between winter and summer. In the summer stratosphere, the highest temperatures are found over the sunlit summer pole and thermal-wind balance then implies westward flow at stratospheric altitudes. Under these conditions Rossby waves forced in the troposphere, which are generally stationary or may even propagate towards the east (in the case of synoptic-scale waves), cannot propagate (Charney and Drazin 1961), and the summer stratosphere is relatively quiescent. In the winter stratosphere, in contrast, the absence of solar heating at the pole implies very low temperatures, an equatorward temperature gradient, and strong eastward flow around the pole (the

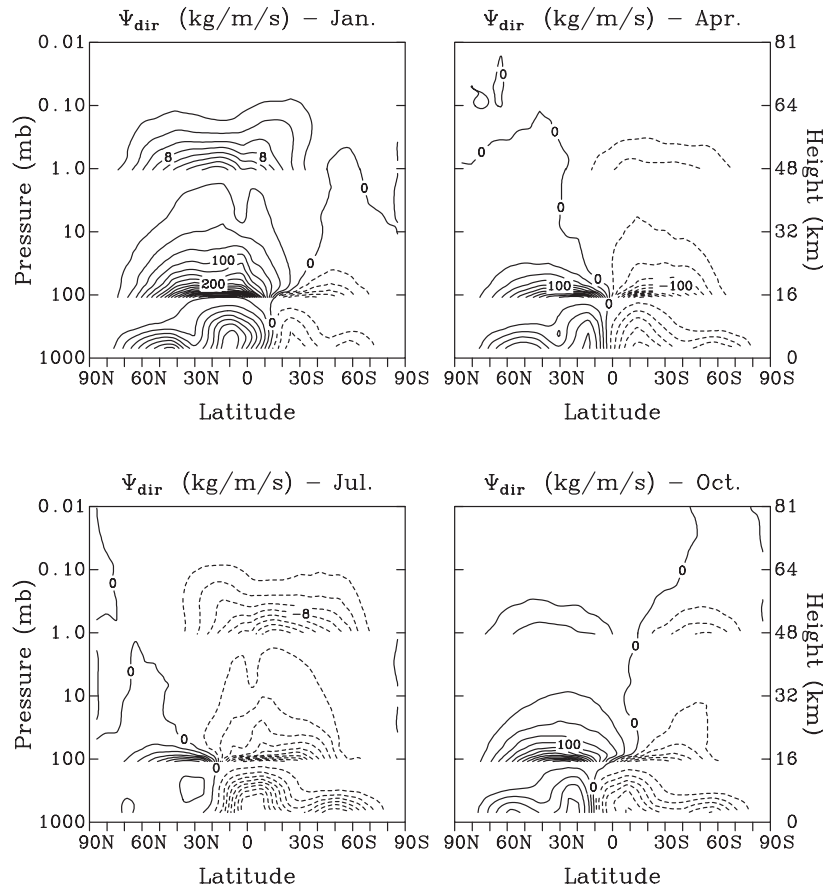


Fig. 3. Mass (TEM) streamfunction for the four cardinal months taken from an integration of the Canadian Middle Atmosphere Model, a comprehensive middle atmosphere climate simulation model. A different set of contour intervals is used in different regions so that the middle atmosphere circulation can be seen. Solid lines indicate counter-clockwise circulation, dashed contours clockwise. Contour intervals are $500 \text{ kg m}^{-1}\text{s}^{-1}$ between 1000 and 100 hPa; $25 \text{ kg m}^{-1}\text{s}^{-1}$ between 100 and 1 hPa; and $2 \text{ kg m}^{-1}\text{s}^{-1}$ above 1 hPa. Evident are the poleward circulations in the lowest part of the stratosphere in both hemispheres; the deep poleward circulation in the winter stratosphere; and the pole-to-pole solstitial circulation in the mesosphere. Reprinted with permission from Beagley et al. (1997), copyright Canadian Meteorological and Oceanographic Society.

“polar vortex”). This situation allows the propagation of planetary-scale Rossby waves into the winter stratosphere (Charney and Drazin 1961) which, like their synoptic-scale cousins, drive a poleward circulation.

The poleward flow in the stratosphere arising from both synoptic-scale and planetary-scale Rossby wave drag implies upwelling in the tropical lower stratosphere and downwelling in the extratropics (Holton et al. 1995). This is the basic explanation for the “Brewer-Dobson circulation”, inferred long ago from observations of

water vapor (Brewer 1949) and ozone (Dobson 1956) and depicted in Fig. 1 during Northern Hemisphere (NH) winter. The implication is that air enters the stratosphere exclusively in the tropics. Air rising through the cold tropical tropopause is dehydrated by freeze drying, but thereafter dehydrates no more as it moves into the warmer stratosphere. Since tropical tropopause temperatures exhibit a pronounced annual cycle (Yulaeva et al. 1994), with lowest temperatures in boreal winter, air passing through the tropical tropopause is dehydrated

most in boreal winter and least in austral winter. This leads to the vertically propagating signal of the “tropical tape recorder” (Mote et al. 1996) seen in Fig. 2, which allows an estimation of an ascent rate of about $0.2\text{--}0.4\text{ mm s}^{-1}$ (fastest in boreal winter, slowest in austral winter).

In addition to Rossby waves, gravity waves propagate from the troposphere into the middle atmosphere. Gravity waves grow exponentially with altitude and will dissipate when they reach a sufficiently large amplitude to break, but will in any case dissipate at a critical level where the phase speed (which is conserved as the waves propagate) matches the background wind speed. In the winter hemisphere, the eastward wind shear implies that eastward-propagating waves encounter critical levels in the lower stratosphere and are removed, leaving only the westward-propagating waves which break in the upper mesosphere and exert a negative drag there. In the summer hemisphere, the opposite applies. Hence in the mesosphere one expects equatorward flow in the summer hemisphere and poleward flow in the winter hemisphere. Together this leads to a summer-to-winter pole circulation, with upwelling over the summer pole and downwelling over the winter pole.

All these features are evident in the Transformed Eulerian Mean (TEM) representation of the Brewer-Dobson circulation (Andrews et al. 1987) shown in Fig. 3, from the Canadian Middle Atmosphere Model (CMAM) (Beagley et al. 1997).

3. Mixing and the distribution of long-lived tracers

In addition to the mean meridional circulation driven by wave dissipation, wave motion induces two-way transport which leads to mixing. (The term ‘mixing’ will be used here to refer to the combined process of two-way transport by fluid motion and the molecular diffusion that ultimately makes the transport irreversible.) In the stratosphere, wave motion is approximately adiabatic and so mixing is mainly quasi-horizontal, along isentropic surfaces. This quasi-horizontal mixing acts to flatten out the latitudinal tracer gradients that would otherwise be steepened by differential vertical motion. The resulting distributions of long-lived

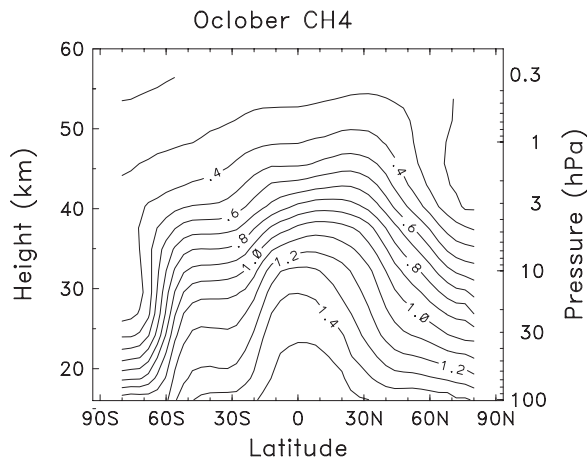


Fig. 4. Latitude-height cross-section of CH_4 mixing ratio for October, in parts per million by volume, from a climatology produced from the HALOE and CLAES instruments on the UARS satellite. The data set is described in Randel et al. (1998). As CH_4 is emitted at the Earth’s surface and destroyed in the stratosphere by oxidation, high values of CH_4 correspond to air that has only recently entered the stratosphere, while low values correspond to air that has been chemically aged. Figure courtesy of Bill Randel, National Center for Atmospheric Research. Reprinted with permission from Shepherd (2003), copyright American Chemical Society.

species exhibit the characteristic shape seen in Fig. 4 for CH_4 , bulging upwards in the tropics and downwards in the extratropics because of the Brewer-Dobson circulation, but maintained in a quasi-steady state by mixing. This distribution is approximately the same for all long-lived species, as they are all affected in the same way by transport; only their vertical gradients differ, depending on their chemical lifetime.

This similar distribution of long-lived species is also true locally and instantaneously, because short-term fluctuations (associated with waves) necessarily preserve the concentrations of long-lived species. Thus, correlations between long-lived species remove the variability associated with short-term fluctuations (Ehhalt

et al. 1983); in contrast, spatial profiles would inevitably exhibit bumps and wiggles associated with these fluctuations. Figure 5 shows the correlation between N_2O and CH_4 from the CMAM and from the very limited measurements made by the ATMOS instrument on board the space shuttle. The full correlation plot from the model, which covers the entire NH stratosphere, is seen to be quite compact; thus, even very limited measurements can span correlation space quite effectively and provide an “instant climatology” (see Fig. 10 of Sankey and Shepherd 2003 for an illustration).

The compactness of the $\text{N}_2\text{O}:\text{CH}_4$ correlation is the result of mixing—note that there is no chemical link between N_2O and CH_4 —but the correlation slope (which corresponds to the relative rates at which the two species decay with height) reflects their chemical lifetimes (Plumb and Ko 1992). Another correlation often studied is that between N_2O and NO_y . Although NO_y is produced from N_2O , this in itself would only lead to an overall negative correlation between NO_y and N_2O (because the conversion is incomplete, and depends on many factors), not to the compact correlation actually found in the lower stratosphere; the compactness again results from mixing. Finally, if one of the species is not particularly long-lived (e.g., ozone, which has a lifetime shorter than the characteristic mixing timescale of a few weeks everywhere except in the lower stratosphere and when isolated in polar night), then its relation to a long-lived species is not compact. This is illustrated by Fig. 6. The CMAM $\text{NO}_y:\text{O}_3$ correlation over the entire NH spans a broad region of $\text{NO}_y:\text{O}_3$ space, reflecting the fact that the ozone distribution (Fig. 1) is not well correlated with that of long-lived species (Fig. 4). As a result, limited sampling of the correlation structure mainly reflects the sampling itself, and may falsely suggest a compactness that is an artifact of the limited sampling (Sankey and Shepherd 2003). The triangles in Figs. 6b and 6d indicate vertical profiles from ATMOS taken at different latitudes, and are completely different from the horizontal profile from the ER-2 aircraft shown in Fig. 6c.

There is a classical description of stratospheric transport (Andrews et al. 1987), based on small-amplitude “mixing length” theory, which consists of a mean meridional circulation

and eddy diffusion. The appeal of this description is its universality: the same mean circulation and eddy diffusivities apply to all tracers, with the tracer-specific aspects of transport residing entirely in the tracer gradients. In this theory, the mean circulation can be shown to equal the (eddy-driven) TEM circulation, under fairly strong assumptions (Dunkerton 1978). While this theory was used in the 1980s to formulate zonal-mean models of middle atmosphere chemical distributions, it did not prove to be of much use in quantitative diagnosis of transport, and has largely been superseded because the mixing-length hypothesis—namely that the length scale of parcel motions is much smaller than that over which the zonal-mean tracer fields vary—is so clearly violated in the stratosphere, at least in the horizontal (see Sections 4 and 5). However the overall framework still remains of conceptual value, and detailed comparisons in realistic situations have shown the vertical component of the Lagrangian mean circulation to be well approximated by that of the TEM circulation (Pendlebury and Shepherd 2003).

Estimates of vertical diffusivity (e.g., from breaking gravity waves) in the lower stratosphere inferred from measurements of tracer structure range from $0.01 \text{ m}^2\text{s}^{-1}$ (Balluch and Haynes 1997) to $0.1 \text{ m}^2\text{s}^{-1}$ (Legras et al. 2005). Sparling et al. (1997) estimated the effective vertical diffusivity resulting from the differential diabatic heating of neighboring air parcels to be $0.1\text{--}0.2 \text{ m}^2\text{s}^{-1}$. A diffusivity κ induces a diffusive flux with a propagation speed w_d that depends on the length scale h according to $w_d \sim \kappa h^{-1}$. For $\kappa \sim 0.2 \text{ m}^2\text{s}^{-1}$, w_d is comparable to a characteristic mean vertical advection speed of $w \sim 0.2 \text{ mm s}^{-1}$ for length scales of $h \sim 1 \text{ km}$, and is an order of magnitude smaller for $h \sim 10 \text{ km}$. Since typical vertical length scales of mean tracer distributions in the stratosphere are $\sim 10 \text{ km}$ or larger (see Fig. 4), this means that vertical diffusion is negligible compared with the vertical component of the TEM circulation in determining the overall meridional structure of tracer distributions.

On the other hand, the latitudinal component of the TEM circulation is proportional to the potential vorticity (PV) flux, and is thus intimately related to eddy mixing. For this reason, latitudinal transport is dominated by eddy mix-

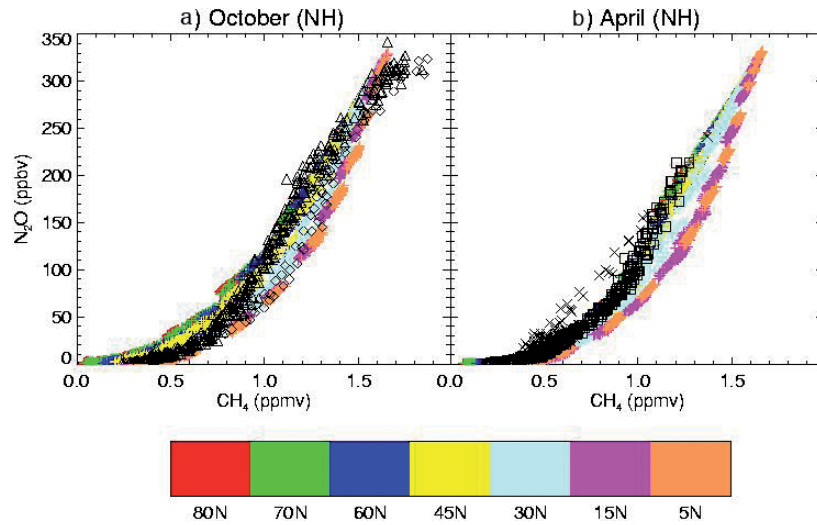


Fig. 5. Scatterplot of N_2O versus CH_4 in the Northern Hemisphere for October and April, from a simulation with the Canadian Middle Atmosphere Model. The color-coding shows the latitude at which the vertical sections were taken. In the vertical the data lie between 100 hPa and 0.3 hPa. The compactness of the correlations is the result of mixing, which leads to spatial distributions like those in Fig. 4 for all long-lived species. The black symbols represent ATMOS measurements from Plate 2 of Michelsen et al. (1998), with diamonds showing tropical data, squares showing midlatitude data, triangles high-latitude data, and crosses vortex data. Reprinted with permission from Sankey and Shepherd (2003), copyright American Geophysical Union.

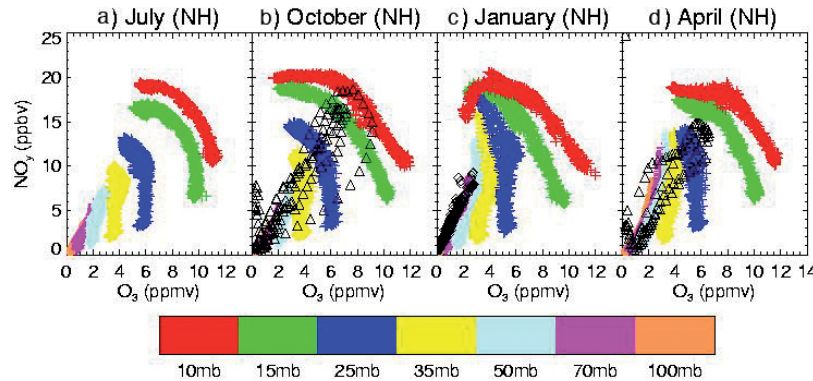


Fig. 6. Scatterplot of NO_y versus O_3 in the Northern Hemisphere for July, October, January and April, from a simulation with the Canadian Middle Atmosphere Model. The color-coding shows the altitude at which the horizontal sections were taken, which span from equator to pole. In contrast to the $N_2O:CH_4$ scatterplots shown in Fig. 5, these scatterplots are not compact. Thus, limited measurements will only sample a part of the overall correlation pattern, and their structure will reflect the nature of the sampling. The ATMOS data [from Fig. 5 of Michelsen et al. (1998)], shown by the triangles in panels (b) and (d), are composed of vertical profiles, and are nearly perpendicular to the model sections at fixed altitude over 10–35 mb. In contrast, the ER-2 aircraft data [from Fig. 3 of Murphy et al. (1993)], shown by the diamonds in panel (c), are taken at a fixed altitude in the lower stratosphere, and are seen to closely follow the model correlation structure at a fixed altitude. Reprinted with permission from Sankey and Shepherd (2003), copyright American Geophysical Union.

ing rather than by the latitudinal component of the TEM circulation (Pendlebury and Shepherd 2003), and most interpretations of stratospheric transport (e.g., Plumb 2002) therefore simplify the picture to one of vertical TEM circulation together with horizontal mixing. At this point there is no general theoretical approach to horizontal mixing in the stratosphere, but some special cases are discussed in Section 5.

A diagnostic encompassing both vertical circulation and horizontal mixing that has proven to be very powerful is that of “age of air”. The concept has applications in many different contexts (see Waugh and Hall 2002) but in the case of the stratosphere refers to the time a parcel of air has spent in the stratosphere since entering it across the tropical tropopause. If the stratospheric circulation consisted only of the Brewer-Dobson circulation, then air would age steadily as it moved upward, poleward and finally downward, and the oldest air would be found in the polar lower stratosphere. However because of mixing, air parcels do not retain their integrity indefinitely and a given volume of air possesses a distribution of ages, corresponding to the various paths with different transit times that brought air to that location (Kida 1983).

Age of air is a theoretical concept which is species-independent, and the age distribution cannot be directly measured. However it turns out that the mean of the age distribution (the “mean age”) is equal to the time lag of a given value of the mixing ratio, relative to the tropical tropopause, for a linearly increasing long-lived tracer (Hall and Plumb 1994). Hence mean age can be estimated from measurements of tracers such as SF₆ and CO₂. Further constraints on the age distribution can be found from the seasonal cycle (e.g., of CO₂ or H₂O). High precision is needed for these measurements, however, and the most extensive estimates of mean age have been obtained from aircraft measurements in the lower stratosphere, at about 22 km altitude (Andrews et al. 2001). These suggest that mean age is around 3 years in midlatitudes and reaches up to about 4–5 years in the highest latitudes in winter. Balloon estimates suggest that mean age can reach 6 years in the high-latitude upper stratosphere (Waugh and Hall 2002). The spatial dis-

tribution of mean age in the CMAM is shown in Fig. 7.

4. Stirring and small-scale structure

Horizontal mixing in the stratosphere arises mainly from breaking Rossby waves: synoptic-scale waves in the lowest part of the subtropical stratosphere, and planetary-scale waves in the deep stratosphere. Being near-adiabatic and balanced, the breaking is “sideways” (McIntyre and Palmer 1983; Jukes and McIntyre 1987) and generates filamentary structure in tracer fields (Waugh et al. 1994). An example from the tropopause region is shown in Fig. 8. Filamentary structure reflects the stirring that is characteristic of two-dimensional velocity fields dominated by large-scale structure (Pierrehumbert 1991; see also Shepherd et al. 2000). Because the stirring is controlled by the large-scale flow, the filamentary structure is predictable (at least over time scales of a few days) from meteorological analyses in the extratropical lower stratosphere, where the large-scale wind fields are reasonably reliable. This has been confirmed by in-situ aircraft measurements in this region (Waugh et al. 1994), and is also reflected in Fig. 8. Horizontal profiles (e.g., taken by an aircraft) of long-lived tracers generically contain such filaments, seen in step-function-like features in tracer concentration (Strahan and Mahlman 1994). Because the horizontal motion varies with altitude, the filaments are vertically sheared and vertical profiles (e.g., taken by an ozonesonde) generically contain so-called “laminae” (Orsolini et al. 1995).

As the stratosphere is, for the most part, dynamically stable, the stirring is not due to some kind of instability but is, rather, forced by Rossby waves propagating up from the troposphere which break in the stratosphere. The breaking phenomenon can be understood in terms of Rossby-wave critical-layer theory (Haynes 2003): where the phase velocity of the wave matches the mean wind velocity, the wave is inevitably nonlinear and the combined effect of the wave and mean flow (in the frame of reference moving with the wave) leads to a hyperbolic stagnation point and a “cat’s eye” structure in the streamfunction field. Such a flow geometry efficiently generates filamentary structure in tracer fields (Pierrehumbert 1991).

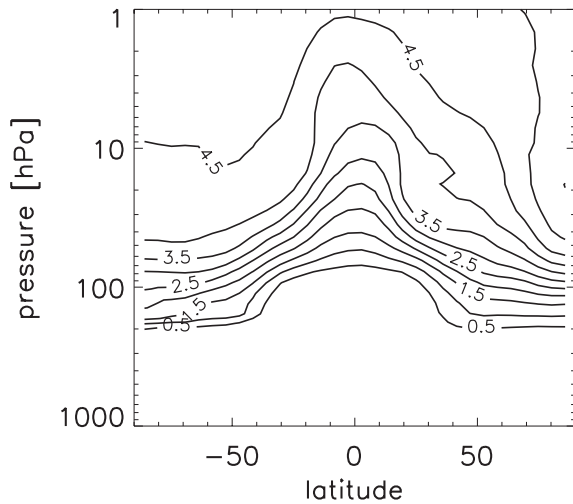


Fig. 7. Annual and zonal mean distribution of mean age of air (in years) within the stratosphere from the Canadian Middle Atmosphere Model, for current conditions. Note the strong resemblance to the distribution of CH₄ shown in Fig. 4. This version of the CMAM is that analyzed in Eyring et al. (2006). Figure courtesy of Michaela Hegglin, University of Toronto.

In the lower stratosphere, synoptic-scale waves encounter critical layers on the subtropical flank of the jet stream (Randel and Held 1991). In the deep stratosphere, planetary-scale waves are generally stationary and the zero wind line represents a critical line. But planetary wave amplitudes are large enough that the critical layer fills the entire midlatitudes, forming what has been called the “stratospheric surf zone” (McIntyre and Palmer 1983). Although a well-defined cat’s eye structure may not always be identifiable, the formation of hyperbolic stagnation points from planetary-scale disturbances is a prerequisite for filamentation of the polar vortex (Polvani and Plumb 1992).

Even a periodic time dependence in the velocity field will lead to chaotic tracer motion in the critical-layer geometry (Ngan and Shepherd 1997a). More generally, conditions in the extratropical stratosphere are such that the correlation time of velocity gradients is much shorter in the Lagrangian reference frame (e.g., following a tracer filament) than in the Eulerian reference frame (Ngan and Shepherd 1999; see Fig. 9). This set-up leads to spatially coherent stirring, with elongated filaments which reflect

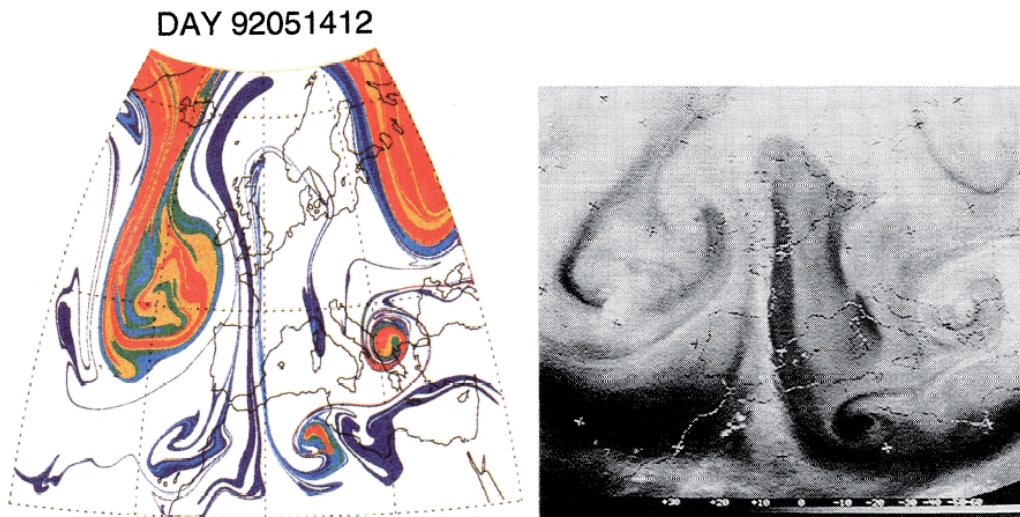


Fig. 8. (a) Contour advection calculation on the 320 K isentropic surface (which crosses the tropopause), initialized from the analyzed potential vorticity (PV) field. The colors denote high values of PV and indicate stratospheric air; the white regions indicate tropospheric air. The stirring of PV contours arises from synoptic-scale disturbances and leads to large-scale deformations of the tropopause as well as filamentation. In this way, large-scale wind fields can lead to small-scale tracer structure. (b) Meteosat water vapor image valid at the same time as panel (a), which confirms that the small-scale structure predicted by the model is real. Reprinted with permission from Appenzeller et al. (1996), copyright American Geophysical Union.

the persistence of the velocity-field structure. Haynes and Anglade (1997) showed that under typical stratospheric conditions the filaments develop a horizontal/vertical aspect ratio as they lengthen and thin which is approximately given by the ratio of the buoyancy frequency to the Coriolis parameter, so about 250. The lengthening and thinning cannot go on forever, and is ultimately limited by vertical mixing which is expected from breaking gravity waves and other small-scale processes, and can be expected to be diffusive. The combination of horizontal strain, vertical shear and vertical diffusion leads to an effective horizontal diffusion. Aircraft measurements of horizontal tracer structure have thus been used to infer the vertical diffusivity in the lower stratosphere (around 22 km altitude), with estimates ranging from around $0.01 \text{ m}^2\text{s}^{-1}$ (Balluch and Haynes 1997) to $0.1 \text{ m}^2\text{s}^{-1}$ (Legras et al. 2005).

Whilst PV is stirred along with chemical tracers, dissipation of PV filamentary structure can occur through radiative damping, which has a strong scale dependence. Haynes and Ward (1993) estimated the importance of this effect and argued that the PV structure could be erased by radiative damping before the chemical structure was erased by vertical mixing, leaving filamentary chemical “fossils” with no dynamical signature.

The filamentary nature of small-scale tracer structure is reflected in tracer spectra. As illustrated in Fig. 8, large-scale stirring rapidly brings into close proximity air masses from different regions, e.g., polar air can be found side-by-side with subtropical air (Waugh et al. 1994). This leads to sharp jumps in horizontal profiles (Strahan and Mahlman 1994), and Ngan and Shepherd (1997b) argued that the approximately k^{-2} variance spectrum found in aircraft measurements of N_2O (Bacmeister et al. 1996), where k is the horizontal spatial wavenumber, reflected the presence of these sharp jumps associated with filamentation. However to complete the argument one must bring in the finite filament lifetime in a self-consistent model (Haynes and Vanneste 2004).

As altitude increases, the relative importance of the gravity-wave component of the velocity field increases. Reliable global estimates of gravity-wave amplitudes from measurements are not available, but general considerations

predict an approximately exponential increase of gravity-wave amplitude with altitude through the stratosphere and lower mesosphere, and this is borne out in the gravity-wave field resolved in middle atmosphere climate models (Koshyk et al. 1999). The models furthermore show an approximately $k^{-5/3}$ horizontal kinetic energy spectrum associated with the gravity waves, which is consistent with aircraft measurements in the lower stratosphere (Bacmeister et al. 1996). However for the scales resolved in the global models this gravity-wave spectrum only emerges distinctly at mesospheric heights. The shallow slope of this spectrum, together with the short timescales associated with gravity waves, fundamentally changes the nature of the horizontal mixing (Shepherd et al. 2000). In particular, the Lagrangian and Eulerian correlation times both become identical and very short as one moves from the middle stratosphere to the lower mesosphere (Fig. 9). Lukovich and Shepherd (2005) studied this process using an idealized model and showed how the presence of gravity waves affects the stirring by planetary waves and leads to a more diffusive horizontal transport. It can also be expected that in the mesosphere the vertical mixing from gravity-wave breaking becomes much more important.

5. Mixing barriers

Horizontal mixing in the stratosphere is spatially inhomogeneous. This can already be seen in Fig. 4, where the CH_4 contours exhibit strong latitudinal gradients in the subtropics and at the edge of the polar vortex at about 60°S . Strong latitudinal gradients of long-lived tracers suggest an inhibition to horizontal mixing, often called a “mixing barrier”.

That such structure exists should not be surprising. The stratospheric surf zone results from breaking planetary waves, and produces strong stirring within a latitude band determined by the fluid dynamics of the nonlinear critical layer. This will inevitably act to homogenize tracer concentrations within the surf zone and create sharp gradients on either side of the surf zone, which represent mixing barriers. Because the stirring also acts on PV, the PV field develops a similar structure, which tends to reinforce the mixing barriers (Juckes and McIntyre 1987). Pendlebury and Shepherd (2003)

quantified the impact of such a structure on the properties of Lagrangian transport. On the poleward side, the critical layer is limited by the strong PV gradient of the polar night jet. On the equatorward side, the situation is more complicated. Polvani et al. (1995) argued that the formation of a subtropical mixing barrier requires strong diabatic relaxation in the tropics, to prevent the surf zone from spreading across the equator. Such a relaxation could come from the tropically confined meridional circulation driven by the latitudinal gradient of radiative heating across the equator during solstice seasons (Dunkerton 1989; Semeniuk and Shepherd 2001a). Exactly what creates the strong latitudinal tracer gradients in the *summer* subtropics is not clear. It is possible that it arises from the tropically-confined solstitial meridional circulation and the mixing arising from the associated inertial adjustment (Semeniuk and Shepherd 2001b), but this has yet to be quantitatively assessed.

The polar vortex mixing barrier has been long recognized (e.g., Juckes and McIntyre 1987) for its importance in creating the chemical isolation needed to produce the Antarctic ozone hole. The extent of the isolation is illustrated by the CMAM results shown in Fig. 10; close inspection of the pattern in midlatitudes reveals cat's eye structures. In the tropics, some degree of isolation is required for the tape-recorder signal to survive over more than one period (Fig. 2), and is also clearly evident in the aerosol observations shown in Fig. 11. The confinement of the aerosol to the tropics for such a long period after the Mount Pinatubo volcanic eruption is unambiguous evidence of a subtropical mixing barrier, at least above about 22 km (Trepte and Hitchman 1992). The evident outflow centred around 20 km (see also Rosenlof et al. 1997) suggests the presence of subtropical eddy mixing at these altitudes, consistent with the strong poleward flow seen in the TEM circulation of Fig. 3 in what is often called the "tropical transition region".

Sparling (2000) has advocated the use of probability distribution functions (PDFs) to quantify mixing regions and mixing barriers: the former are associated with maxima in tracer-concentration PDFs, the latter with minima. The advantage of using PDFs over mean tracer gradients is that they are less sensitive

to outliers and hence to the effect of intrusions, which can shift means. An example is shown in Fig. 12 from CLAES measurements of N_2O in the upper stratosphere. Neu et al. (2003) use this method to quantify the seasonal evolution and vertical structure of the subtropical mixing barrier. An alternative and complementary approach avoids the use of tracer measurements altogether but uses winds to drive an off-line passive tracer field and thereby compute "effective diffusivity" (Haynes and Shuckburgh 2000); this approach also is effective at identifying the subtropical and polar-vortex mixing barriers as minima in effective diffusivity.

Mixing barriers are the reason why the application of mixing-length theory (and horizontal eddy diffusivity) is so problematical in the stratosphere (see Pierrehumbert 1991). Theoretical approaches to mixing across the barrier regions have thus tended to assume the extreme limit of exchange between well-defined "reservoirs". Such approaches can never be global but they can at least provide some local information. For example, Plumb (1996) proposed a "tropical pipe" model of stratospheric transport, which identified distinct tropical and extratropical air masses with distinct correlations between long-lived species (as can be seen in Fig. 5). Such a model—generalized to include lateral exchange—can be used in combination with tracer measurements to infer exchange rates across the edge of the pipe (Volk et al. 1996), to estimate vertical diffusion within the pipe (Hall and Waugh 1997), and to understand the distribution of age of air (Neu and Plumb 1999). In the context of the polar vortex, isolation allows the development of distinct tracer-tracer correlations within the vortex, although mixing across the vortex edge can complicate the interpretation of their time evolution (Plumb et al. 2000).

6. The UTLS

So far the discussion has mainly focused on the deep stratosphere, above the altitude of the tropical tropopause (approximately 18 km, typically characterized as the 380 K isentropic surface). Because the tropopause slopes downward as one moves away from the equator, reaching an altitude of roughly 8 km at the highest latitudes, there is a significant part of the strato-

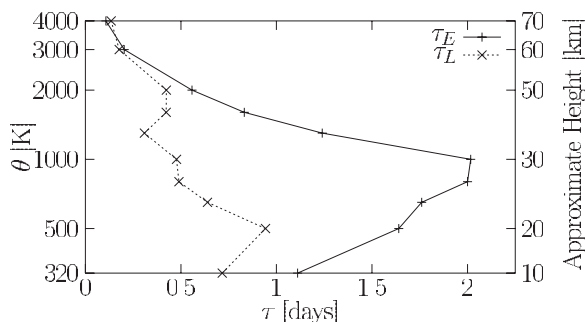


Fig. 9. Eulerian (τ_E) and Lagrangian (τ_L) correlation times of horizontal velocity shears versus potential temperature (and approximate height), computed from isentropic winds from the Canadian Middle Atmosphere Model. In the stratosphere, τ_L is much shorter than τ_E , which is the setting for chaotic advection and leads to the characteristic filamentary structure seen in the stratosphere. In the mesosphere, τ_L and τ_E become comparable and both become very short, limited only by the numerics of the model. The dramatic change with altitude reflects the dominance of gravity-wave motion in the mesosphere. Reprinted with permission from Shepherd et al. (2000), copyright American Geophysical Union.

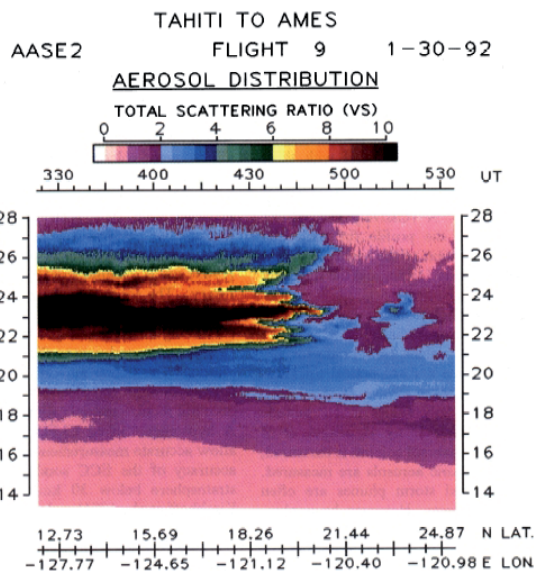
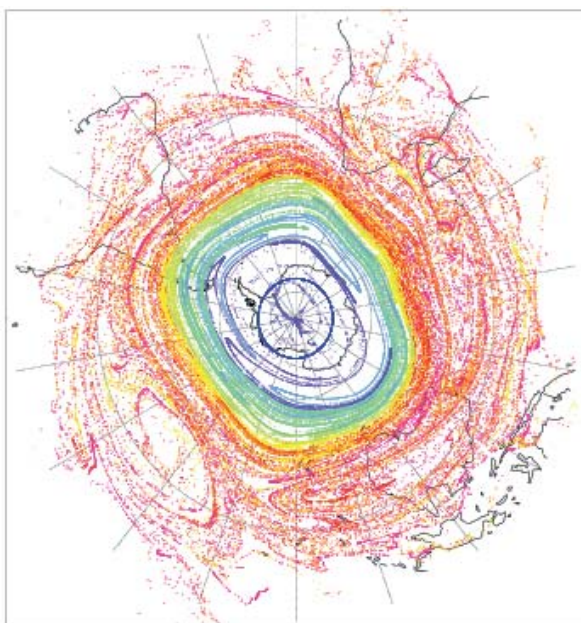


Fig. 11. Aerosol distribution observed from an airborne lidar seven months after the eruption of the Mount Pinatubo volcano. The cross-section was taken in the West Pacific across the northern subtropics. Above about 22 km altitude, the strong confinement of the aerosol to the tropics (equatorward of about 20°N) provides direct evidence of the subtropical mixing barrier that defines the “tropical pipe”. Below 22 km, there is more rapid transport to midlatitudes. Reprinted with permission from Grant et al. (1994), copyright American Geophysical Union.

Fig. 10. Results of a 30-day particle advection calculation using isentropic winds at 450 K (approximately 17 km altitude), in the heart of the wintertime polar ozone layer, from the Canadian Middle Atmosphere Model for a model July. The particles were initially located along rings of constant latitude, with each ring indicated with a different color. Note the strong isolation of the polar vortex, compared to the mixing in the surf zone outside. Figure courtesy of Keith Ngan, University of Toronto. Reprinted with permission from Shepherd (2000), copyright Elsevier Science.

Dec 3, 1992 – Jan 6, 1993

6.8 mb

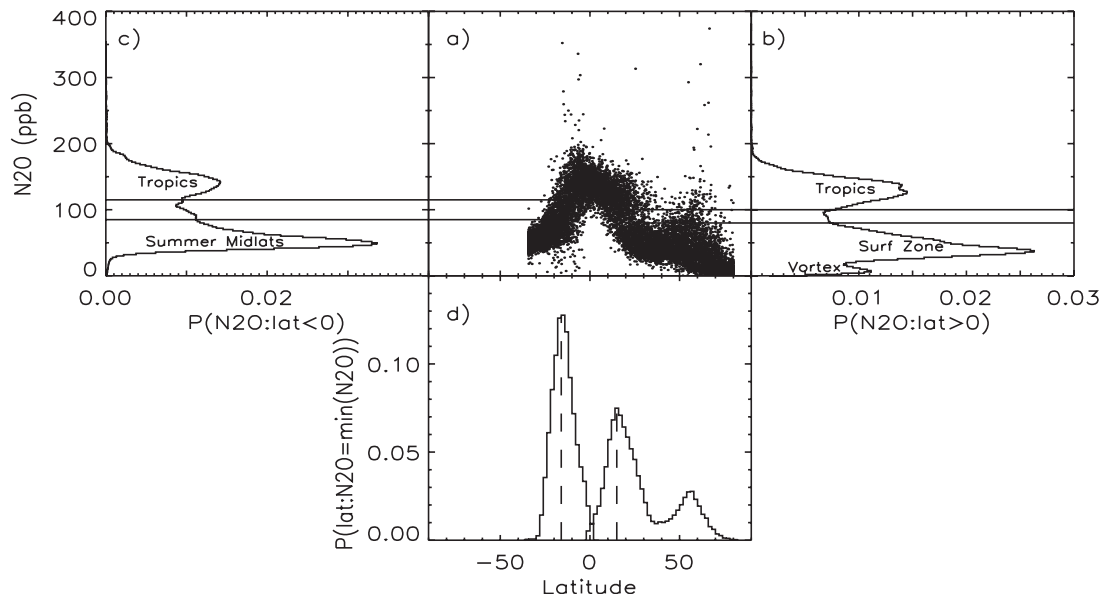


Fig. 12. (a) Scatterplot of CLAES N₂O measurements versus latitude in the upper stratosphere during NH winter. (b) PDF of N₂O in the NH. (c) PDF of N₂O in the SH. The valley in the PDFs between the tropics and midlatitudes, indicated by the horizontal lines, corresponds to the strong N₂O gradient in the subtropics and reflects the subtropical mixing barrier. The polar vortex mixing barrier is also evident in the NH. (d) PDF of the latitudes of the measurements lying within each subtropical valley. The subtropical mixing barrier is identified with the most probable latitude in each hemisphere, indicated by the vertical dashed lines. Reprinted with permission from Neu et al. (2003), copyright American Geophysical Union.

sphere below the 380 K isentropic surface—dubbed the “lowermost stratosphere” by Holton et al. (1995). In this region, isentropic surfaces pass through the tropopause, potentially allowing for rapid stratosphere-troposphere exchange. The upper part of the tropical troposphere is likewise a distinguished region, as the top of the region of moist convective adjustment, at about 12 km altitude, lies well below the tropical tropopause, and the layer in between is in many ways more characteristic of the stratosphere than of the troposphere (Thurn and Craig 2002). Together these two regions are now generally referred to as the UTLS. The UTLS is deserving of special treatment because its properties are in many ways quite distinct from those of the main body of the stratosphere, yet are also distinct from the lower troposphere (Haynes and Shepherd 2001).

The tropical part of the UTLS is known as the tropical tropopause layer (TTL), although there is no consensus on its exact definition (Haynes and Shepherd 2001). The significance of the TTL was noted long ago (Palmén and Newton 1969) and has been revived several times since (e.g., Highwood and Hoskins 1998). The wave-induced Brewer-Dobson upwelling must reach down into the TTL, but will at some level be overwhelmed by tropospheric processes. This is seen in the sign of the clear-sky radiative heating, which changes from positive above about 15 km to negative below. From the perspective of transport it is probably preferable to consider the level of zero clear-sky radiative heating as the base of the TTL, as then the outflow from convective towers will tend to remain in the TTL and air can become chemically aged before it crosses the tropical tropopause.

A simple model of convective uplift followed by slow diabatic upwelling and photochemical production seems to account quite well for the observed vertical profile of ozone in the tropics (Folkins et al. 1999), which does not exhibit a sharp transition at the tropopause but rather increases gradually with altitude throughout the TTL. Indeed, the tropical tropopause itself has no particular significance for transport, except insofar as the cold point is significant for tropical dehydration and thus for transport of water vapor into the stratosphere. Hence one might reasonably consider the base of the tropical pipe, rather than the tropical tropopause, as the top of the UTLS (Rosenlof et al. 1997). There is much current interest in transport within the TTL because of its importance in chemical aging and dehydration. A key issue for chemical aging is the extent to which the TTL is isolated, and the residence time within it (Fueglistaler et al. 2004). A key issue for dehydration is the lowest temperature experienced by an air parcel as it passes through the tropical tropopause. Fueglistaler et al. (2005) argue, on the basis of trajectory calculations, that this (together with saturation at 100% relative humidity over ice) is enough to quantitatively explain observed stratospheric humidity levels, without the need to invoke mesoscale or detailed cloud microphysical processes. However studies of transport in the TTL are currently limited by the poor quality of the tropical winds (especially the vertical motion) in meteorological analyses, and by uncertainties in convective transport.

In the extratropical (stratospheric) part of the UTLS, the Brewer-Dobson circulation is persistently downward. This controls the flux of many chemical species, including lower-stratospheric ozone, into the troposphere (Holton et al. 1995). Although the Brewer-Dobson downwelling must continue into the troposphere, mixing timescales are much more rapid in the troposphere than in the stratosphere. This leads to a strong contrast in concentrations of species with moderate lifetimes such as ozone (high in the stratosphere, low in the troposphere), water vapor and CO (high in the troposphere, low in the stratosphere).

The role of the extratropical tropopause in shaping tracer concentrations is evident from the ACE-FTS satellite data shown in Fig. 13.

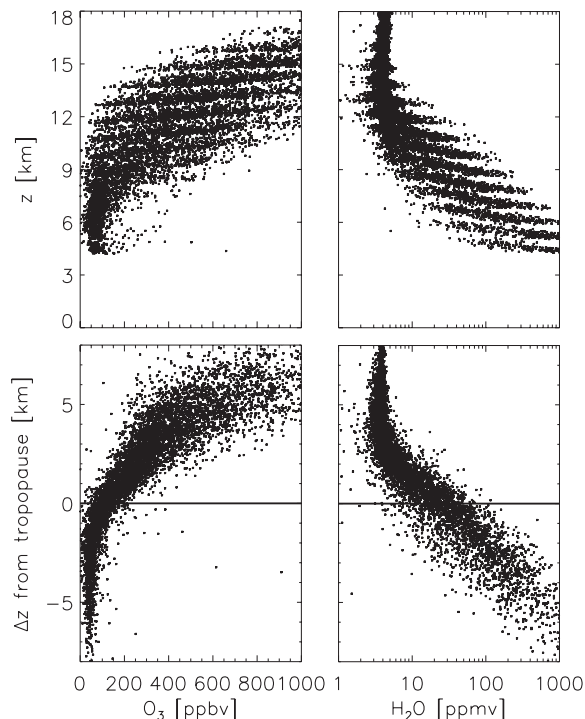


Fig. 13. Vertical profiles of O_3 (left panels) and H_2O mixing ratios (right panels) obtained from the Canadian ACE-FTS satellite instrument (see Bernath et al. 2005; Boone et al. 2005; Walker et al. 2005) for spring measurements during 2005 and 2006 at latitudes between 40° and $60^\circ N$. The profiles are depicted as a function of altitude (top panels) and of altitude relative to the thermal tropopause (bottom panels). The data illustrate the role of the tropopause in shaping tracer distributions in the tropopause region. In particular, a strong gradient in tracer mixing ratios across the tropopause is revealed by the tropopause-based coordinate system. Figure courtesy of Michaela Hegglin, University of Toronto.

Plotted against geometric altitude, ozone generally increases with altitude while water vapor generally decreases; but plotted relative to the height of the thermal tropopause, the profiles tend to cluster and indicate a sharper transition between tropospheric and stratospheric values. Yet as Fig. 13 also makes clear, the transition is not abrupt and occurs across a region several km deep which exhibits both tro-

ospheric and stratospheric chemical characteristics. In particular, ozone does not reach characteristic tropospheric values until almost 1 km below the tropopause (lower left panel), a fact noted a decade ago by Bethan et al. (1996) from ozonesonde measurements. On the other hand water vapor does not reach characteristic stratospheric values until about 2 km above the tropopause (lower right panel). The latter applies also to CO, and this extratropical transition region was first identified from simultaneous aircraft measurements of ozone and CO (Fischer et al. 2000). The transition region may well be related to the tropopause inversion layer identified by Birner (2006) from high-vertical-resolution temperature profiles, as the vertical scales are comparable, although this has yet to be established.

The extratropical tropopause is alternatively identified by a sharp horizontal gradient in PV along isentropic surfaces (Hoskins et al. 1985). While a strong PV gradient should in principle create an impediment to horizontal transport, the PV tropopause is regularly forced to meander wildly by synoptic-scale baroclinic disturbances, as seen in Fig. 8. These meanders can break (Postel and Hitchman 1999), leading to irreversible stratosphere-troposphere exchange, and even when they do not break will be subject to diabatic processes which can lead to stratosphere-troposphere exchange. It has been argued that this process of Rossby-wave breaking is in fact responsible for the sharpness of the extratropical tropopause (Haynes et al. 2001).

Whilst the importance of stratosphere-to-troposphere downward transport associated with tropopause folds has been long recognized (Danielson 1968), tropopause folds are just the vertical manifestation of PV stirring (Hoskins et al. 1985) and it is clear from Fig. 8 and from general fluid-dynamical considerations that the exchange must in fact be two-way. This is confirmed by in-situ tracer measurements in the lowermost stratosphere (Ray et al. 1999). In addition to this quasi-isentropic transport, there is direct evidence of diabatic troposphere-to-stratosphere transport in midlatitudes from intense convective events (Poulida et al. 1996; Hegglin et al. 2004).

Thus, one may generically expect to see the influence of recently tropospheric air just above

the tropopause, and of recently stratospheric air just below, leading to a transition layer in the relevant trace species. That the transition layer appears to be much thicker on the stratospheric side of the tropopause (Fig. 13) is to be expected based on the drastically different mixing timescales within the troposphere and stratosphere. In the troposphere, the impact of stratospheric intrusions will be rapidly mixed away; while in the stratosphere, the impact of tropospheric intrusions has to compete only with the much slower Brewer-Dobson downwelling. In this way, symmetric two-way exchange across the tropopause would lead to an asymmetric transition region. This effect has been quantified by Hegglin et al. (2005).

Because the PV tropopause meanders so wildly, measurements of chemical species taken at a given location will vary greatly depending on the position of the PV tropopause relative to that location. Much of this variability can be removed by plotting fields in terms of “equivalent latitude”, which is a scaled PV coordinate (Butchart and Remsberg 1986). In this way, measurements taken at a single latitude sample a wide range of equivalent latitudes. The concept of equivalent latitude was first introduced to deal with deformations of the polar vortex. While the concept extends in principle to the tropopause region, there are issues in practice because equivalent latitude is not well defined where PV gradients are weak, and the accuracy of PV in meteorological analyses may be suspect (see Birner et al. 2006). Moreover tracers in the tropopause region tend not to be as uniform along PV contours as they are in the polar vortex, because the PV tropopause is not as effective a mixing barrier as is the polar vortex: the PV deformations are generally much more extensive and irreversible, and so air parcels cannot be expected to circumnavigate the PV tropopause several times around the globe, as they are observed to do along the polar vortex edge (cf., Fig. 10).

Nevertheless PV together with potential temperature offers a quasi-Lagrangian coordinate system which can be used to represent tracer cross-sections in the UTLS (Hoor et al. 2004). There is a marked seasonal cycle associated with the strong seasonal cycle of the Brewer-Dobson downwelling (Hegglin et al. 2006). During winter and spring tracers indicate more of a

deep stratospheric origin, while during summer and fall they reflect transport directly into the UTLS from the tropical transition region (see Fig. 11). The same inferences can also be made from tracer-tracer correlations (Boering et al. 1994; Ray et al. 1999), which provide an alternate means of removing short-term dynamical variability.

7. Interannual variability and transport of ozone

If the Brewer-Dobson circulation is mainly driven by drag associated with breaking Rossby waves, and horizontal mixing is mainly determined by the same process of Rossby-wave breaking, then it follows that interannual variations in stratospheric transport will be associated with variations in Rossby-wave forcing. There are various mechanisms for such variability. The generation of Rossby waves in the troposphere will vary from year to year, reflecting the variability of the troposphere itself. Much of this variability is certainly associated with variations in sea-surface temperatures, e.g., El Niño, but even models with annually repeating sea-surface temperatures exhibit interannual variability. Since the location of the stratospheric surf zone depends on the location of the zero-wind line, which depends on the phase of the Quasi-Biennial Oscillation (QBO) (Holton and Tan 1980), the QBO provides another source of stratospheric dynamical variability—even in the extratropics. Natural variability can also arise from external forcings such as volcanic eruptions and solar variability.

Water vapor is a special case. In the tropical lower stratosphere, just as the annual cycle of tropical tropopause temperature is apparent in the seasonal tape recorder (Fig. 2), so too is interannual variability of tropopause temperature apparent in interannual anomalies in the tape recorder signal (Fig. 14).

Within the tropics the QBO has a direct effect on tracer variability, partly associated with the circulation anomalies induced along with the QBO (Hasebe 1994), and partly by the QBO modulation of the semi-annual oscillation (SAO), which affects tracer distributions in the tropical upper stratosphere and lower mesosphere (Randel et al. 1998). In fact the QBO is the dominant factor in the interannual variability of tropical ozone (Bowman 1989), the

second most important being the 11-year solar cycle. Since these variations are essentially periodic in time, they are relatively easy to isolate in time series and to distinguish from long-term trends. However in the extratropics the natural variability is primarily associated with variations in Rossby-wave forcing, so is non-periodic and cannot be easily distinguished from long-term trends. It is thus important to understand the causes of interannual variability in stratospheric transport associated with Rossby-wave forcing, and its effect on long-term ozone changes.

The effect of interannual variability on total ozone can be clearly seen in the seasonal cycle of ozone in different years (Fig. 15). In midlatitudes, ozone increases from late fall through to early spring as a result of transport by the Brewer-Dobson circulation (Fig. 1), and then declines from late spring through early fall once the stratospheric winds become easterly, the deep branch of the Brewer-Dobson circulation shuts down (Fig. 3), and ozone is destroyed photochemically. However the amplitude (and to a lesser extent the shape) of the seasonal cycle varies from year to year, as the wave forcing varies (Fusco and Salby 1999; Randel et al. 2002). In the same way, the larger wintertime build-up, on average, in the NH as compared with the SH results from the stronger planetary-wave drag in the former; note that the late-summer ozone values are very comparable in the two hemispheres.

If the seasonal build-up of ozone can vary from year to year because of variations in wave drag, then long-term changes in wave drag imply long-term changes in the seasonal build-up of ozone and, hence, in ozone abundance not just in winter and spring but throughout the summer. This is important to understand and quantify because it needs to be distinguished from the effects of ozone-depleting substances. The contribution of changes in stratospheric wave drag to midlatitude ozone changes is very sensitive to the exact time period chosen, because of the strong interannual variability of wave drag, but estimates for the time period 1979–2000 suggest that up to 30% of the NH midlatitude ozone decline can be attributed to changes in wave drag and thus to changes in transport (Randel et al. 2002).

Similar considerations apply to long-term

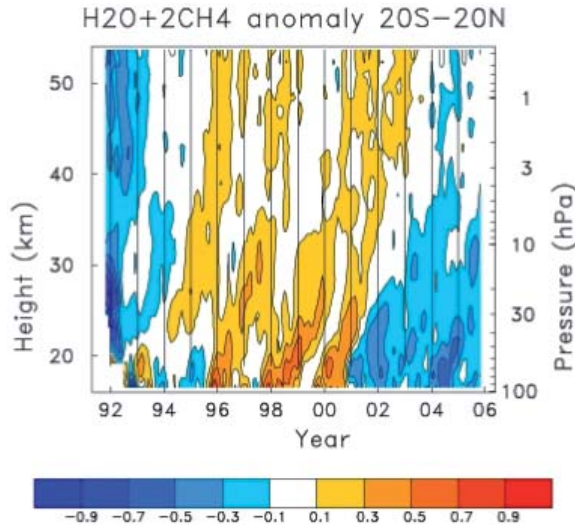


Fig. 14. Time-height cross-section of interannual anomalies in “total water” (twice methane plus water) in the tropics, in parts per million by volume and zonally averaged between 20°S and 20°N, using data from the HALOE instrument on UARS. Total water is conserved in the presence of methane oxidation so enables the tape recorder signal to be followed up to the stratopause. The differences in total water before and after 2000 are coherent with the differences in tropical tropopause temperature (Randel et al. 2004). Figure courtesy of Bill Randel, National Center for Atmospheric Research.

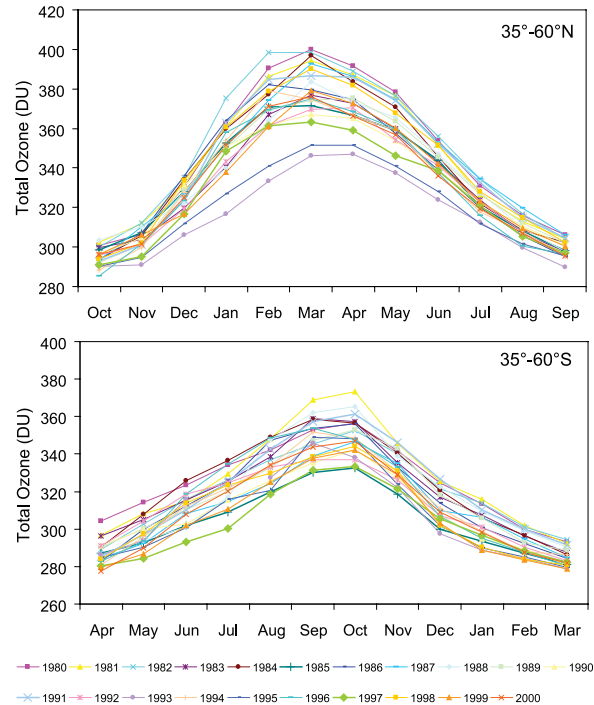


Fig. 15. Area-weighted total ozone, expressed in Dobson Units (DU), over (a) 35°–60°N and (b) 35°–60°S. Each curve denotes a different year between 1980 and 2000. The winter-spring buildup from transport and summertime decline from photochemical loss are evident. Years with high ozone values in late spring are seen to remain high through the summer. Reprinted with permission from Fioletov and Shepherd (2003), copyright American Geophysical Union.

ozone changes in the Arctic, which exhibit strong decadal variability (Fig. 16). Chemical ozone loss is modulated by meteorological variability, but cold winters are cold because of a weaker circulation and thus are also associated with less ozone transport into polar regions. Hence chemical ozone loss and ozone transport tend to act in concert, with roughly an equal contribution (since the early 1990s) to interannual variability of total ozone within the Arctic vortex (Rex et al. 2004). Another way to say this is that the natural variability in Arctic ozone that would occur from transport has been amplified by a factor of two by chemical ozone loss. In the Antarctic, dynamics also influences the year-to-year variability of total ozone (Fig.

16) but the development of the ozone hole during the 1980s was certainly the result of the buildup of ozone-depleting substances.

Fioletov and Shepherd (2003) showed that in the NH, the long-term trends in summertime midlatitude ozone are slaved to the springtime trends in the same way that summertime anomalies are slaved to the springtime anomalies. In other words, the seasonality of ozone trends is explained by the seasonality of ozone anomalies. It follows that up to 30% of the NH summertime ozone trends (over 1979–2000) can be traced to changes in winter-spring transport.

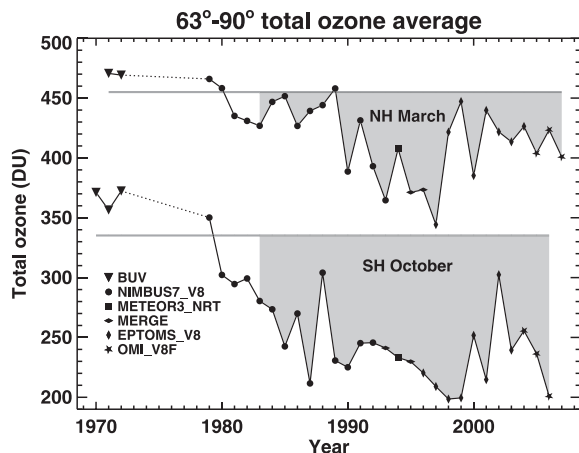


Fig. 16. Average column ozone poleward of 63° latitude in the springtime of each hemisphere, in Dobson units (DU), based on data from various satellite instruments as indicated. The ozone hole in the Antarctic is apparent. In contrast, the very low values seen in the Arctic in the 1990s arose from meteorological variability, and resulted from a combination of the reduced ozone transport and enhanced chemical ozone loss associated with a more confined and colder polar vortex in those years. Figure courtesy of Paul Newman, NASA Goddard Space Flight Center, updated from Newman et al. (1997).

In the SH, uncertainties in the quantification of long-term changes in wave forcing prevent an assessment of the role of transport changes in the long-term ozone decline. However in the SH, transport plays another role. When the vortex breaks down in late spring, transport of ozone-depleted air from polar regions into midlatitudes has a significant impact on midlatitude ozone levels, increasing the ozone loss from what would be expected based on photochemical decay of the springtime midlatitude losses, and leading to a relatively weak seasonality of the long-term ozone decline (Fioletov and Shepherd 2005). Rapid combination of polar and midlatitude ozone anomalies after the vortex breakdown occurs in both hemispheres, but in the NH the long-term polar ozone decline is sufficiently small that its effect on the long-term midlatitude ozone decline is difficult to discern.

8. Transport in models

Models are important tools for understanding atmospheric processes and for the detection, attribution and prediction of changes associated with particular forcings. It is thus important to determine how well models represent stratospheric transport. In this respect it is necessary to distinguish between free-running chemistry climate models (CCMs) and chemistry transport models (CTMs) driven by meteorological analyses. (Two-dimensional zonal-mean models are not considered here.)

We first consider CCMs, which are general circulation models with interactive chemistry. There are two issues: the representation of the relevant dynamical processes in the models, and the numerical representation of transport. With respect to the former, the main issue is whether the wave-driven circulation and wave-induced mixing are correct. Because the relevant features are mainly large-scale, they should in principle be reasonably well represented in any climate model with a sufficiently high lid, provided the tropospheric climate is reasonable. The impact on the wave-driven circulation is evident in the temperature field, so if the latter is reasonable then the former should not be too far wrong. Nevertheless there remain a number of ways in which the dynamics in CCMs could produce incorrect transport.

First, there is considerable uncertainty in the circulation induced by gravity-wave drag, which is not well constrained by measurements and which varies considerably between models. This will affect the temperature and hence strength of the polar vortex (Garcia and Boville 1994), and thus the extent of vortex isolation. CCMs have a systematic bias in that the Antarctic vortex breaks down too late (Eyring et al. 2006); this will inevitably lead to errors in the mixing between polar regions and midlatitudes during the late-spring/early-summer period in the SH. Second, if a CCM does not represent the QBO—and most do not—then the tropical winds will be persistently easterly and this will affect the location of the stratospheric surf zone and the strength of the subtropical mixing barriers. Persistent tropical easterlies may also be the origin of the systematic problem found in some CCMs where the Arctic is perpetually “disturbed” and does not exhibit the extremely

cold winters found in nature (Austin et al. 2003); such models will then not exhibit signatures of Arctic isolation in chemical fields (Sankey and Shepherd 2003; witness the lack of a distinct vortex branch to the $\text{N}_2\text{O}:\text{CH}_4$ correlation in Fig. 5b in the model). Third, significant aspects of mesospheric dynamics such as the SAO and the two-day wave, which have major implications for transport, depend on the model's representation of equatorially trapped waves and gravity waves and thus could easily be unrealistic. It is important to recognize errors in transport that, like these, result from an underlying deficiency in the model dynamics.

The second issue for transport in CCMs involves the model numerics. An obvious statement is that the model lid must be high enough to allow the necessary transport to take place. Because the Brewer-Dobson circulation involves the upper stratosphere, it is not possible to achieve realistic age of air in the lower stratosphere (and hence, e.g., inorganic chlorine loading) unless a model well resolves the upper stratosphere (Eyring et al. 2006). In practice this means a lid in the lower mesosphere, at least at 0.1 hPa, because the upper scale height of a model must be devoted to a sponge layer to prevent spurious reflection of waves at the model lid. Similar considerations apply for studies of solar variability, since the effect of solar variability on ozone occurs in the upper stratosphere. For a proper representation of polar ozone there is strong evidence that transport of NO_x from the mesosphere can be important (Randall et al. 2001), which would also argue for a lid placed well into the mesosphere. The strong descent of air from the mesosphere into the polar vortex during winter is evident in Fig. 3.

Because of the slow vertical transport time-scales in the stratosphere, artificial vertical diffusion can be a factor in models. As noted earlier, the vertical diffusivity associated with subgrid-scale motion could be as large as $0.1 \text{ m}^2\text{s}^{-1}$ in the lower stratosphere (Legras et al. 2005), yet would still be an order of magnitude weaker than the vertical advection associated with the Brewer-Dobson circulation over a vertical scale of 10 km. If in a model the diffusivity were instead set to $1 \text{ m}^2\text{s}^{-1}$ for numerical reasons, then the two effects would become comparable, with the numerical diffusion

perhaps even dominant in the summer hemisphere where the Brewer-Dobson circulation is so weak. Unpublished analysis of the CMAM shows that the vertical profiles of long-lived species in the late summer were greatly improved when the vertical diffusivity was decreased from 1 to $0.1 \text{ m}^2\text{s}^{-1}$ (S. Melo, personal communication, 2004). Also the summertime persistence of ozone anomalies, which is quite realistic in CMAM for a vertical diffusivity of $0.1 \text{ m}^2\text{s}^{-1}$, is rapidly lost for $1 \text{ m}^2\text{s}^{-1}$ (Tegtmeier and Shepherd 2007).

Finally, there is the issue of the advection algorithm itself. Spectral advection has been much criticized because of its spatially nonlocal properties, but it conserves species automatically and its negative effects can be mitigated in the stratosphere by the use of chemical families to reduce spatial gradients of advected species. Jockel et al. (2001) argue that it is most important to have consistency between mass advection in the dynamical core and the tracer advection scheme, otherwise tracer number densities will not be conserved; so for spectral dynamical cores, this argues for spectral advection. Semi-Lagrangian schemes (e.g., Williamson and Rasch 1989) have been widely used but are known to be overly diffusive (Eluszkiewicz et al. 2000), which is an issue for the representation of mixing barriers in the stratosphere. In principle the most accurate transport scheme would seem to be finite-volume or flux-form (Lin and Rood 1996), at least in terms of reducing spurious diffusion. However a recent comparison of transport properties in CCMs (Eyring et al. 2006) found that there was little difference in key transport diagnostics between models with spectral and flux-form advection. It seems that the errors associated with spectral advection do not accumulate, and thus do not lead to serious bias problems, although this has yet to be confirmed.

Earlier comparisons of tracer transport in stratospheric models (e.g., Hall et al. 1999) found that models were seriously deficient, with too young age of air and too rapid vertical propagation of the tropical tape recorder. However the most recent comparison (Eyring et al. 2006) shows that many models have quite reasonable age of air (Fig. 17)—if still a little young—and that the tape recorder ascent is likewise reasonable—if still a little too rapid.

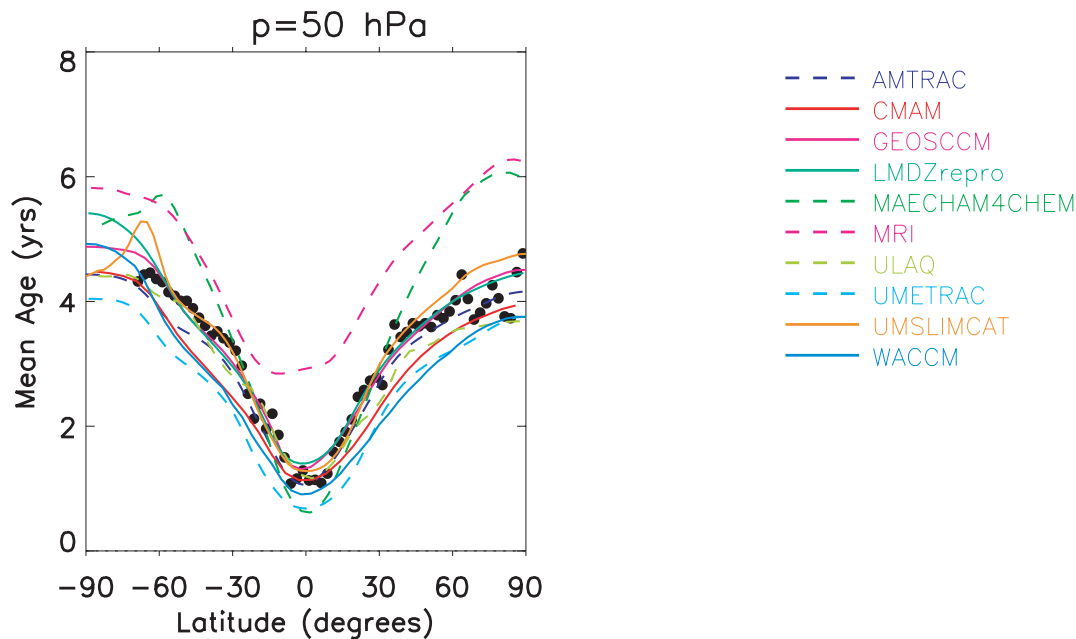


Fig. 17. Mean age of air at 50 hPa from various CCMs (colors) and as estimated from aircraft measurements (black dots). Most of the models shown exhibit a fairly realistic distribution of age of air, although there is a general tendency for the ages to be slightly too young. Reprinted with permission from Eyring et al. (2006), copyright American Geophysical Union.

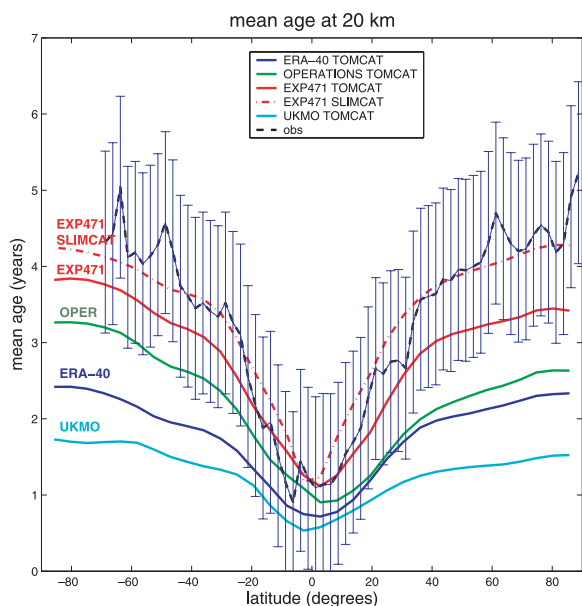


Fig. 18. Mean age of air at 20 km altitude from TOMCAT and SLIMCAT CTM calculations using different ECMWF and UKMO analyses for the year 2000, as indicated. The observed estimates are derived from aircraft measurements and include 2σ error bars. “Oper” indicates the ECMWF operational analysis, while “EXP471” indicates the latest ECMWF “interim” reanalysis. As the analyses improve, age of air increases and the gap between TOMCAT and SLIMCAT narrows (see also Chipperfield 2006). Reprinted with permission from Monge-Sanz et al. (2007), copyright American Geophysical Union.

Probably the main reason for improvement is just the increase in spatial resolution (both horizontal and vertical) that has occurred in the latest generation of CCMs, and further improvements can be expected as resolution continues to improve.

CTMs are usually driven by winds from meteorological analyses. This removes most of the errors associated with the representation of dynamics (e.g., the absence of a QBO or a strong-vortex bias), while retaining those associated with model numerics, but introduces other very significant sources of error. The noise introduced by the assimilation process can lead to spurious horizontal and vertical dispersion, and the lack of consistency between the radiation field and the vertical motion can lead to errors in the Brewer-Dobson circulation. These problems can potentially undermine the use of CTMs for long-term integrations, such as in quantifying the impact of transport changes on ozone depletion (Chipperfield 2003).

Studies of transport properties in CTMs driven by analyses have indeed suggested that transport is much too dispersive, and age of air therefore much too young at middle and high latitudes (Schoeberl et al. 2003). Using forecast rather than analyzed winds reduces the dispersion (Meijer et al. 2004), as does the use of shorter intervals between analyses (Legras et al. 2005). These findings suggest that the spurious dispersion found by using analysed winds at 6-hour intervals results from effectively “freezing” the noise introduced in the assimilation process, introducing artificially long correlation times in the winds by interpolating between 6-hour intervals. This is analogous to the spurious latitudinal dispersion found by Shepherd et al. (2000) when mesospheric fields in CMAM were sampled too infrequently (thus artificially increasing the correlation times) to resolve the transport associated with gravity waves. To address the problem of a too-fast Brewer-Dobson circulation, the preferred strategy has been to dispense with the vertical motion field from the analysis and instead use isentropic coordinates and compute the diabatic motion from an independent radiation code (e.g., Chipperfield 2003). The problem with that approach, however, is that any bias in the radiation code will translate into a persistent bias in the diabatic transport; for a

CCM, in contrast, a bias in the radiation code will translate only into a bias in temperature, not transport, since for a CCM the diabatic transport is controlled by wave forcing.

As data assimilation systems improve, both bias and noise are reduced, and one may therefore expect an improvement in the transport properties of analyzed winds. This is reflected in the mean age of air obtained from ECMWF analyses as shown in Fig. 18. The SLIMCAT CTM uses isentropic coordinates and diabatic vertical transport, while the TOMCAT CTM uses sigma coordinates and winds calculated from the analyses. As the assimilation system has improved the mean age of air in TOMCAT has systematically increased (compare the solid curves), with furthermore a tightening of the gradient between the tropics and midlatitudes. Moreover the gap between SLIMCAT and TOMCAT has narrowed (Chipperfield 2006). Although the exact reasons for the improvements are not known, they are believed to result from a reduction in both bias and noise (Monge-Sanz et al. 2007). Results such as this offer great encouragement that analyzed winds may finally become useful for studies of long-term transport.

9. Final remarks

Twenty-five years ago, the subject of middle atmosphere transport was in its infancy. The Brewer-Dobson circulation had been inferred 30 years earlier from measurements of ozone and water vapor, and confirmed in early satellite measurements of long-lived species, but had been a puzzle until the theoretical breakthrough in the late 1970s provided by the TEM circulation (Andrews and McIntyre 1976) and its relation to tracer transport (Dunkerton 1978). This work fundamentally explained the poleward sense of the Brewer-Dobson circulation, and its wave-driven (not radiatively-driven) nature, concepts subsequently refined in the notions of “downward control” (Haynes et al. 1991) and the “wave-driven pump” (Holton et al. 1995). However the mixing aspects of tracer transport were at that time based on small-amplitude, mixing-length theory. While this led to a rather beautiful theoretical framework (see Andrews et al. 1987), it was shattered almost at birth by the discovery of the stratospheric surf zone (McIntyre and Palmer

1983). In particular, the sharp mixing barriers created by coherent large-scale stirring create a situation opposite to that required for the application of mixing-length theory (Pierrehumbert 1991).

This issue became one of much more than academic importance with the discovery of the Antarctic ozone hole in the mid 1980s. The mixing barrier associated with the polar vortex edge was quickly understood to be an essential ingredient in setting up the conditions for severe chemical ozone loss. Furthermore stratospheric transport was long understood to be crucial for determining the lifetime of ozone-depleting substances and the availability of inorganic chlorine. Thus, the rapid development of research on stratospheric ozone depletion following the discovery of the ozone hole provided a major impetus for research on stratospheric transport. This happily coincided with the availability of widespread satellite measurements of trace species, especially from the UARS satellite launched in 1991, as well as high-altitude aircraft measurements specially dedicated to understanding ozone depletion. The 1990s thus represented something of a golden age for research in stratospheric transport. Kinematic studies of transport driven by winds from meteorological analyses proved remarkably successful in reproducing observed features in tracer fields, such as sharp gradients and filamentary structure (Waugh et al. 1994), spurring the widespread use of such methods (illustrated here by Figs. 8, 9 and 10).

In the last few years, the focus in research on transport has evolved from short-term (days to weeks) to long-term (years to decades), driven by the recent emergence of CCMs as useful tools for attribution and prediction of stratospheric changes. Scientifically this development dovetails with the evolution of the ozone-depletion problem to one involving chemistry-climate coupling. At the same time, it seems that stratospheric meteorological analyses are just about reaching the point where they can provide useful products for studies of long-term transport. This should enable CTMs to finally realize their potential for attributing past ozone changes. In fact, accuracy of winds for transport studies is now regarded as an important metric for the quality of stratospheric analyses. In the next 5–10 years, it can be anticipated

that CCM and CTM studies will enter their own golden age and refine the quantitative understanding of stratospheric transport. At the same time, data assimilation systems encompassing the stratosphere will begin to incorporate chemical data assimilation in a fully interactive manner, and understanding transport errors in these chemical analyses will be a major concern.

Quite apart from the technical developments, three scientific frontiers are apparent. The first is in the tropical stratosphere. Our understanding of transport in the extratropical stratosphere has been greatly aided by the availability of reliable wind fields (reliable, at least, for studies of short-term transport) from meteorological analyses, but these winds are mainly derived from satellite temperature measurements by virtue of the strong balance constraints that exist in the extratropical stratosphere. In the tropics, the coupling between winds and temperature is much weaker and the quality of the wind fields in analyses is therefore much poorer (SPARC 2002; Polavarapu and Shepherd 2006). However, the planned SWIFT satellite instrument (see Polavarapu and Shepherd 2006) will provide direct measurements of horizontal winds (and ozone fluxes) from 15–55 km altitude, which should significantly advance our understanding of transport in the tropical stratosphere.

A second frontier is the UTLS region, which is emerging as a nexus of chemistry-climate coupling (Haynes and Shepherd 2001) where transport plays a crucial role. A challenge here is the fine horizontal and vertical scales involved; to resolve the mean structure of chemical and dynamical fields around the tropopause requires a spatial resolution of at least 100 km in the horizontal and 1 km in the vertical. Accordingly the primary sources of quantitative information in this region up to now have been measurements from aircraft and sondes. However there is new information now becoming available from satellite instruments with good vertical resolution (e.g., the ACE-FTS data shown in Fig. 13), thereby allowing for global coverage, and one may anticipate further improvements in satellite measurements of key species (especially water vapor and ozone) in the future. Model resolution is likewise improving to the point where CCMs can

be expected to start providing a reasonable representation of the UTLS. As CCMs begin to simulate the entire troposphere-stratosphere system, the role of the UTLS in chemistry-climate coupling is sure to develop as a major research focus in climate science, with transport as a central aspect.

Finally, the mesosphere remains largely unexplored in comparison with the stratosphere. Whilst there has long been considerable interest in the MLT region, the region below (50–80 km) has been largely ignored. Yet the mesosphere provides an important upper boundary condition for the stratosphere, and any serious consideration of the role of solar variability in climate must encompass this region. As one moves from the stratosphere into the mesosphere, the nature of the large-scale circulation changes (Fig. 3) but also the dynamics becomes more complicated: timescales become much faster (Fig. 9) because of the increasing dominance of gravity waves, vertical mixing from gravity-wave breaking becomes much more important, and disturbances are no longer solely forced but can arise from in-situ instabilities such as the two-day wave. As both CCMs and data assimilation systems raise their lids to encompass the mesosphere we can expect increasing attention to be paid to transport processes in this region.

Acknowledgements

The author is grateful to Thomas Birner, Peter Haynes, Michaela Hegglin, Peter Hitchcock, Kirstin Krüger, Beatriz Monge-Sanz, Susann Tegtmeier, Darryn Waugh, and two anonymous reviewers, for comments which led to improvements in the manuscript, and to Diane Pendlebury for help with the figures. Support is acknowledged from the Natural Sciences and Engineering Research Council of Canada, the Canadian Foundation for Climate and Atmospheric Sciences, and the Canadian Space Agency. The ACE-FTS data is shown courtesy of Peter Bernath, Chris Boone, Kaley Walker and the ACE Science Team; ACE is supported by the Canadian Space Agency.

References

- Andrews, A.E., K.A. Boering, S.C. Wofsy, B.C. Daube, D.B. Jones, S. Alex, M. Loewenstein, J.R. Podolske, and S.E. Strahan, 2001: Empirical age spectra for the midlatitude lower stratosphere from in situ observations of CO₂: Quantitative evidence for a subtropical “barrier” to horizontal transport. *J. Geophys. Res.*, **106**, 10257–10274.
- Andrews, D.G. and M.E. McIntyre, 1976: Planetary waves in horizontal and vertical shear: the generalized Eliassen-Palm relation and the mean zonal acceleration. *J. Atmos. Sci.*, **33**, 2031–2048.
- Andrews, D.G., J.R. Holton, and C.B. Leovy, 1987: *Middle Atmosphere Dynamics*. Academic Press, 489 pp.
- Appenzeller, C., H.C. Davies, and W.A. Norton, 1996: Fragmentation of stratospheric intrusions. *J. Geophys. Res.*, **101**, 1435–1456.
- Austin, J., D. Shindell, S.R. Beagley, C. Brühl, M. Dameris, E. Manzini, T. Nagashima, P. Newman, S. Pawson, G. Pitari, E. Rozanov, C. Schnadt, and T.G. Shepherd, 2003: Uncertainties and assessments of chemistry-climate models of the stratosphere. *Atmos. Chem. Phys.*, **3**, 1–27.
- Bacmeister, J.T., S.D. Eckermann, P.A. Newman, L. Lait, K.R. Chan, M. Loewenstein, M.H. Proffitt, and B.L. Gary, 1996: Stratospheric horizontal wavenumber spectra of winds, potential temperature, and atmospheric tracers observed by high-altitude aircraft. *J. Geophys. Res.*, **101**, 9441–9470.
- Balluch, M.G. and P.H. Haynes, 1997: Quantification of lower stratospheric mixing processes using aircraft data. *J. Geophys. Res.*, **102**, 23487–23504.
- Barry, L., G.C. Craig, and J. Thuburn, 2002: Poleward transport by the atmospheric heat engine. *Nature*, **416**, 774–777.
- Beagley, S.R., J. de Grandpré, J.N. Koshyk, N.A. McFarlane, and T.G. Shepherd, 1997: Radiative-dynamical climatology of the first-generation Canadian middle atmosphere model. *Atmos.-Ocean*, **35**, 293–331.
- Bernath, P.F., et al., 2005: Atmospheric Chemistry Experiment (ACE): Mission overview. *Geophys. Res. Lett.*, **32**, doi: 10.1029/2005GL022386.
- Bethan, S., G. Vaughan, and S.J. Reid, 1996: A comparison of ozone and thermal tropopause heights and the impact of tropopause definition on quantifying the ozone content of the troposphere. *Quart. J. Roy. Meteor. Soc.*, **122**, 929–944.
- Birner, T., 2006: Fine-scale structure of the extratropical tropopause region. *J. Geophys. Res.*, **111**, D04104, doi: 10.1029/2005JD006301.
- Birner, T., D. Sankey, and T.G. Shepherd, 2006: The tropopause inversion layer in models and analyses. *Geophys. Res. Lett.*, **33**, doi: 10.1029/2006GL026549.

- Boering, K.A., B.C. Daube, S.C. Wofsy, M. Loewenstein, J.R. Podolske, and E.R. Keim, 1994: Tracer-tracer relationships and lower stratospheric dynamics: CO₂ and N₂O correlations during SPADE. *Geophys. Res. Lett.*, **21**, 2567–2570.
- Boone, C.D., R. Nassar, K.A. Walker, Y. Rochon, S.D. McLeod, C.P. Rinsland, and P.F. Bernath, 2005: Retrievals for the Atmospheric Chemistry Experiment Fourier Transform Spectrometer. *Appl. Opt.*, **44**, 7218–7231.
- Bowman, K.P., 1989: Global patterns of the Quasi-Biennial Oscillation in total ozone. *J. Atmos. Sci.*, **46**, 3328–3343.
- Brewer, A.W., 1949: Evidence for a world circulation provided by the measurements of helium and water vapor distribution in the stratosphere. *Quart. J. Roy. Meteor. Soc.*, **75**, 351–363.
- Butchart, N. and E.E. Remsburg, 1986: The area of the stratospheric polar vortex as a diagnostic for tracer transport on an isentropic surface. *J. Atmos. Sci.*, **43**, 1319–1339.
- Charney, J. and P.G. Drazin, 1961: Propagation of planetary-scale disturbances from the lower into the upper atmosphere. *J. Geophys. Res.*, **66**, 83–109.
- Chipperfield, M.P., 2003: A three-dimensional model study of long-term mid-high latitude lower stratosphere ozone changes. *Atmos. Chem. Phys.*, **3**, 1253–1265.
- Chipperfield, M.P., 2006: New version of the TOMCAT/SLIMCAT off-line Chemical Transport Model: Intercomparison of stratospheric tracer experiments. *Quart. J. Roy. Meteor. Soc.*, **132**, 1179–1203.
- Danielsen, E.F., 1968: Stratospheric-tropospheric exchange based on radioactivity, ozone and potential vorticity. *J. Atmos. Sci.*, **25**, 502–518.
- Dobson, G.M.B., 1956: Origin and distribution of the polyatomic molecules in the atmosphere. *Proc. Roy. Soc. Lond. A*, **236**, 187–193.
- Dunkerton, T.J., 1978: On the mean meridional mass motions of the stratosphere and mesosphere. *J. Atmos. Sci.*, **35**, 2325–2333.
- Dunkerton, T.J., 1989: Nonlinear Hadley circulation driven by asymmetric differential heating. *J. Atmos. Sci.*, **46**, 956–974.
- Ehhalt, D.G., E.P. Roth, and U. Schmidt, 1983: On the temporal variance of stratospheric gas concentrations. *J. Atmos. Chem.*, **1**, 27–51.
- Eluszkiewicz, J., R.S. Hemler, J.D. Mahlman, L. Bruhwiler, and L.L. Takacs, 2000: Sensitivity of age-of-air calculations to the choice of advection scheme. *J. Atmos. Sci.*, **57**, 3185–3201.
- Eyring, V., et al., 2006: Assessment of coupled chemistry-climate models: Evaluation of dynamics, transport characteristics and ozone. *J. Geophys. Res.*, **111**, doi: 10.1029/2006JD007327.
- Fioletov, V.E. and T.G. Shepherd, 2003: Seasonal persistence of midlatitude total ozone anomalies. *Geophys. Res. Lett.*, **30**, doi: 10.1029/2002GL016739.
- Fioletov, V.E. and T.G. Shepherd, 2005: Summer-time total ozone variations over middle and polar latitudes. *Geophys. Res. Lett.*, **32**, doi: 10.1029/2004GL022080.
- Fischer, H., F.G. Weinhold, P. Hoor, O. Bujok, C. Schiller, P. Siegmund, M. Ambaum, H.A. Scheeren, and J. Lelieveld, 2000: Tracer correlations in the northern high latitude lowermost stratosphere: Influence of cross-tropopause mass exchange. *Geophys. Res. Lett.*, **27**, 97–100.
- Folkins, I., M. Loewenstein, J. Podolske, S.J. Oltmans, and M. Proffitt, 1999: A barrier to vertical mixing at 14 km in the tropics: Evidence from ozonesondes and aircraft measurements. *J. Geophys. Res.*, **104**, 22095–22102, doi: 10.1029/1999JD900404.
- Fortuin, J.P.F. and H. Kelder, 1998: An ozone climatology based on ozonesonde and satellite measurements. *J. Geophys. Res.*, **103**, 31709–31734.
- Fueglistaler, S., H. Wernli, and T. Peter, 2004: Tropical troposphere-to-stratosphere transport inferred from trajectory calculations. *J. Geophys. Res.*, **109**, D03108, doi: 10.1029/2003JD004069.
- Fueglistaler, S., M. Bonazzola, P.H. Haynes, and T. Peter, 2005: Stratospheric water vapor predicted from the Lagrangian temperature history of air entering the stratosphere in the tropics. *J. Geophys. Res.*, **110**, D08107.
- Fusco, A.C. and M.L. Salby, 1999: Interannual variations of total ozone and their relationship to variations of planetary wave activity. *J. Climate*, **12**, 1619–1629.
- Garcia, R.R. and B.A. Boville, 1994: “Downward control” of the mean meridional circulation and temperature distribution of the polar winter stratosphere. *J. Atmos. Sci.*, **51**, 2238–2245.
- Grant, W.B., et al., 1994: Aerosol-associated changes in tropical stratospheric ozone following the eruption of Mount Pinatubo. *J. Geophys. Res.*, **99**, 8197–8211.
- Hall, T.M. and R.A. Plumb, 1994: Age as a diagnostic of stratospheric transport. *J. Geophys. Res.*, **99**, 1059–1070.
- Hall, T.M. and D. Waugh, 1997: Tracer transport in the tropical stratosphere due to vertical diffusion and horizontal mixing. *Geophys. Res. Lett.*, **24**, 1383–1386.
- Hall, T.M., D.W. Waugh, K.A. Boering, and R.A. Plumb, 1999: Evaluation of transport in strato-

- spheric models. *J. Geophys. Res.*, **104**, 18815–18839.
- Hasebe, F., 1994: Quasi-biennial oscillations of ozone and diabatic circulation in the equatorial stratosphere. *J. Atmos. Sci.*, **51**, 729–745.
- Haynes, P.H., 2003: Critical layers. In *Encyclopedia of Atmospheric Sciences* (ed. J.R. Holton, J.A. Pyle and J.A. Curry), Academic Press.
- Haynes, P. and J. Anglade, 1997: The vertical-scale cascade in atmospheric tracers due to large-scale differential advection. *J. Atmos. Sci.*, **54**, 1121–1136.
- Haynes, P.H., C.J. Marks, M.E. McIntyre, T.G. Shepherd, and K.P. Shine, 1991: On the “downward control” of extratropical diabatic circulations by eddy-induced mean zonal forces. *J. Atmos. Sci.*, **48**, 651–678.
- Haynes, P., J. Scinocca, and M. Greenslade, 2001: Formation and maintenance of the extratropical tropopause by baroclinic eddies. *Geophys. Res. Lett.*, **28**, 4179–4182.
- Haynes, P.H. and T.G. Shepherd, 2001: Report on the SPARC Tropopause Workshop. *SPARC Newsletter*, **17**, 3–10.
- Haynes, P. and E. Shuckburgh, 2000: Effective diffusivity as a diagnostic of atmospheric transport. 1. Stratosphere. *J. Geophys. Res.*, **105**, 22777–22794.
- Haynes, P.H. and J. Vanneste, 2004: Stratospheric tracer spectra. *J. Atmos. Sci.*, **61**, 161–178.
- Haynes, P.H. and W.E. Ward, 1993: The effect of realistic radiative transfer on potential-vorticity structures, including the influence of background shear and strain. *J. Atmos. Sci.*, **50**, 3431–3453.
- Hegglin, M.I., et al., 2004: Tracing troposphere-to-stratosphere transport above a mid-latitude deep convective system. *Atmos. Chem. Phys.*, **4**, 741–756.
- Hegglin, M.I., D. Brunner, T. Peter, J. Staehelin, V. Wirth, P. Hoor, and H. Fischer, 2005: Determination of eddy-diffusivity in the lowermost stratosphere. *Geophys. Res. Lett.*, **32**, L13812, doi: 10.1029/2005GL022495.
- Hegglin, M.I., D. Brunner, T. Peter, P. Hoor, H. Fischer, J. Staehelin, M. Krebsbach, C. Schiller, U. Parchatka, and U. Weers, 2006: Measurements of NO, NO_y, N₂O, and O₃ during SPURT: Implications for transport and chemistry in the lowermost stratosphere. *Atmos. Chem. Phys.*, **6**, 1331–1350.
- Held, I.M. and B.J. Hoskins, 1985: Large-scale eddies and the general circulation of the troposphere. *Advances in Geophys.*, **28A**, 3–31.
- Highwood, E.J. and B.J. Hoskins, 1998: The tropical tropopause. *Quart. J. Roy. Meteor. Soc.*, **124**, 1579–1604.
- Holton, J.R., P.H. Haynes, M.E. McIntyre, A.R. Douglass, R.B. Rood, and L. Pfister, 1995: Stratosphere-troposphere exchange. *Rev. Geophys.*, **33**, 403–439.
- Holton, J.R. and H.-C. Tan, 1980: The influence of the equatorial quasi-biennial oscillation on the global circulation at 50 mb. *J. Atmos. Sci.*, **37**, 2200–2208.
- Hoor, P., C. Gurk, D. Brunner, M.I. Hegglin, H. Wernli, and H. Fischer, 2004: Seasonality and extent of extratropical TST derived from in-situ CO measurements during SPURT. *Atmos. Chem. Phys.*, **4**, 1427–1442.
- Hoskins, B.J., M.E. McIntyre, and A.W. Robertson, 1985: On the use and significance of isentropic potential-vorticity maps. *Quart. J. Roy. Meteor. Soc.*, **111**, 877–946.
- IPCC/TEAP, 2005: Safeguarding the Ozone Layer and the Global Climate System: Issues Related to Hydrofluorocarbons and Perfluorocarbons. *IPCC/TEAP Special Report* (ed. B. Metz et al.), Cambridge University Press, 478 pp.
- Jockel, P., R. von Kuhlmann, M.G. Lawrence, B. Steil, C.A.M. Brenninkmeijer, P.J. Crutzen, P.J. Rasch, and B. Eaton, 2001: On a fundamental problem in implementing flux-form advection schemes for tracer transport in 3-dimensional general circulation and chemistry transport models. *Quart. J. Roy. Meteor. Soc.*, **127**, 1035–1052.
- Jukes, M.N. and M.E. McIntyre, 1987: A high resolution, one-layer model of breaking planetary waves in the stratosphere. *Nature*, **328**, 590–596.
- Kida, H., 1983: General circulation of air parcels and transport characteristics derived from a hemispheric GCM. 2. Very long-term motions of air parcels in the troposphere and stratosphere. *J. Meteor. Soc. Japan*, **61**, 510–523.
- Koshyk, J.N., B.A. Boville, K. Hamilton, E. Manzini, and K. Shibata, 1999: The kinetic energy spectrum of horizontal motions in middle-atmosphere models. *J. Geophys. Res.*, **104**, 27177–27190.
- Legras, B., I. Pisso, G. Berthet, and F. Lefèvre, 2005: Variability of the Lagrangian turbulent diffusion in the lower stratosphere. *Atmos. Chem. Phys.*, **5**, 1605–1622.
- Lin, S.-J. and R.B. Rood, 1996: Multidimensional flux-form semi-Lagrangian transport schemes. *Mon. Wea. Rev.*, **124**, 2046–2070.
- Lukovich, J.V. and T.G. Shepherd, 2005: Stirring and mixing in two-dimensional divergent flow. *J. Atmos. Sci.*, **62**, 3933–3954.
- McIntyre, M.E., 2000: On global-scale atmospheric and oceanic circulations. In *Perspectives in Fluid Dynamics* (ed. G.K. Batchelor, H.K. Mof-

- fat and M.G. Worster), Cambridge University Press.
- McIntyre, M.E. and T.N. Palmer, 1983: Breaking planetary waves in the stratosphere. *Nature*, **305**, 593–600.
- Meijer, E.W., B. Bregman, A. Segers, and P.F.J. van Velthoven, 2004: The influence of data assimilation on the age of air calculated with a global chemistry-transport model using ECMWF wind fields. *Geophys. Res. Lett.*, **31**, L23114.
- Michelsen, H.A., G.L. Manney, M.R. Gunson, and R. Zander, 1998: Correlations of stratospheric abundances of NO_y, O₃, N₂O, and CH₄ derived from ATMOS measurements. *J. Geophys. Res.*, **103**, 28347–28359.
- Monge-Sanz, B.M., M.P. Chipperfield, A.J. Simmons, and S.M. Uppala, 2007: Mean age of air and transport in a CTM: Comparison of different ECMWF analyses. *Geophys. Res. Lett.*, **34**, doi: 10.1029/2006GL028515.
- Mote, P.W., et al., 1996: An atmospheric tape recorder: The imprint of tropical tropopause temperatures on stratospheric water vapor. *J. Geophys. Res.*, **101**, 3989–4006.
- Murphy, D.M., D.W. Fahey, M.H. Proffitt, C.S. Liu, K.R. Chan, C.S. Eubank, S.R. Kawa, and K.K. Kelly, 1993: Reactive nitrogen and its correlation with ozone in the lower stratosphere and upper troposphere. *J. Geophys. Res.*, **98**, 8751–8773.
- Neu, J.L. and R.A. Plumb, 1999: Age of air in a “leaky pipe” model of stratospheric transport. *J. Geophys. Res.*, **104**, 19243–19255.
- Neu, J.L., L.C. Sparling, and R.A. Plumb, 2003: Variability of the subtropical “edges” in the stratosphere. *J. Geophys. Res.*, **108**, 4482.
- Newman, P.A., J.F. Gleason, R.D. McPeters, and R.S. Stolarski, 1997: Anomalously low ozone over the Arctic. *Geophys. Res. Lett.*, **24**, 2689–2692.
- Ngan, K. and T.G. Shepherd, 1997a: Chaotic mixing and transport in Rossby-wave critical layers. *J. Fluid Mech.*, **334**, 315–351.
- Ngan, K. and T.G. Shepherd, 1997b: Comments on some recent measurements of anomalously steep N₂O and O₃ tracer spectra in the stratospheric surf zone. *J. Geophys. Res.*, **102**, 24001–24004.
- Ngan, K. and T.G. Shepherd, 1999: A closer look at chaotic advection in the stratosphere. Part I: Geometric structure. *J. Atmos. Sci.*, **56**, 4134–4152.
- Orsolini, Y.J., P. Simon, and D. Cariolle, 1995: Filamentation and layering of an idealized tracer by observed winds in the lower stratosphere. *Geophys. Res. Lett.*, **22**, 839–842.
- Palmén, E. and C. Newton, 1969: *Atmospheric Circulation Systems*. Academic Press, 603 pp.
- Pendlebury, D. and T.G. Shepherd, 2003: Planetary-wave-induced transport in the stratosphere. *J. Atmos. Sci.*, **60**, 1456–1470.
- Pierrehumbert, R.T., 1991: Large-scale horizontal mixing in planetary atmospheres. *Phys. Fluids A*, **3**, 1250–1260.
- Plumb, R.A., 1996: A “tropical pipe” model of stratospheric transport. *J. Geophys. Res.*, **101**, 3957–3972.
- Plumb, R.A., 2002: Stratospheric transport. *J. Meteor. Soc. Japan*, **80**, 793–809.
- Plumb, R.A. and M.K.W. Ko, 1992: Interrelationships between mixing ratios of long-lived stratospheric constituents. *J. Geophys. Res.*, **97**, 10145–10156.
- Plumb, R.A., D.W. Waugh, and M.P. Chipperfield, 2000: The effects of mixing on tracer relationships in the polar vortices. *J. Geophys. Res.*, **105**, 10047–10062.
- Polavarapu, S. and T.G. Shepherd, 2006: Report on the Joint SPARC Workshop on Data Assimilation and Stratospheric Winds. *SPARC Newsletter*, **26**, 20–27.
- Polvani, L.M. and R.A. Plumb, 1992: Rossby-wave breaking, microbreaking, filamentation, and secondary vortex formation—The dynamics of a perturbed vortex. *J. Atmos. Sci.*, **49**, 462–476.
- Polvani, L.M., D.W. Waugh, and R.A. Plumb, 1995: On the subtropical edge of the stratospheric surf zone. *J. Atmos. Sci.*, **52**, 1288–1309.
- Postel, G.A. and M.H. Hitchman, 1999: A climatology of Rossby wave breaking along the subtropical tropopause. *J. Atmos. Sci.*, **56**, 359–373.
- Poulida, O., R.R. Dickerson, and A. Heymsfield, 1996: Stratosphere-troposphere exchange in a midlatitude mesoscale convective complex. *J. Geophys. Res.*, **101**, 6823–6836.
- Randall, C.E., D.E. Siskind, and R.M. Bevilacqua, 2001: Stratospheric NO_x enhancements in the southern hemisphere vortex in winter/spring of 2000. *Geophys. Res. Lett.*, **28**, 2385–2388.
- Randel, W.J. and I.M. Held, 1991: Phase speed spectra of transient eddy fluxes and critical layer absorption. *J. Atmos. Sci.*, **48**, 688–697.
- Randel, W.J., F. Wu, J.M. Russell III, A. Roche, and J.W. Waters, 1998: Seasonal cycles and QBO variations in stratospheric CH₄ and H₂O observed in UARS HALOE data. *J. Atmos. Sci.*, **55**, 163–185.
- Randel, W.J., F. Wu, and R. Stolarski, 2002: Changes in column ozone correlated with the stratospheric EP flux. *J. Meteor. Soc. Japan*, **80**, 849–862.
- Randel, W.J., F. Wu, S.J. Oltmans, K. Rosenlof, and G.E. Nedoluha, 2004: Interannual changes of stratospheric water vapor and correlations

- with tropical tropopause temperatures. *J. Atmos. Sci.*, **61**, 2133–2148.
- Ray, E.A., F.L. Moore, J.W. Elkins, G.S. Dutton, D.W. Fahey, H. Vomel, S.J. Oltmans, and K.H. Rosenlof, 1999: Transport into the Northern Hemisphere lowermost stratosphere revealed by in situ tracer measurements. *J. Geophys. Res.*, **104**, 26565–26580.
- Rex, M., R.J. Salawitch, P. von der Gathen, N. Harris, M.P. Chipperfield, and B. Naujokat, 2004: Arctic ozone loss and climate change. *Geophys. Res. Lett.*, **31**, doi: 10.1029/2003GL018844.
- Rosenlof, K.H., A.F. Tuck, K.K. Kelly, J.M. Russell III, and M.P. McCormick, 1997: Hemispheric asymmetries in water vapor and inferences about transport in the lower stratosphere. *J. Geophys. Res.*, **102**, 13213–13234.
- Sankey, D. and T.G. Shepherd, 2003: Correlations of long-lived chemical species in a middle atmosphere general circulation model. *J. Geophys. Res.*, **108**, doi: 10.1029/2002JD002799.
- Schoeberl, M.R., A.R. Douglass, Z. Zhu, and S. Pawson, 2003: A comparison of the lower stratospheric age spectra derived from a general circulation model and two data assimilation systems. *J. Geophys. Res.* **108**, doi: 10.1029/2002JD002652.
- Semeniuk, K. and T.G. Shepherd, 2001a: The middle-atmosphere Hadley circulation and equatorial inertial adjustment. *J. Atmos. Sci.*, **58**, 3077–3096.
- Semeniuk, K. and T.G. Shepherd, 2001b: Mechanisms for tropical upwelling in the stratosphere. *J. Atmos. Sci.*, **58**, 3097–3115.
- Shepherd, T.G., 2000: The middle atmosphere. *J. Atmos. Solar-Terres. Phys.*, **62**, 1587–1601.
- Shepherd, T.G., 2003: Large-scale atmospheric dynamics for atmospheric chemists. *Chem. Reviews*, **103**, 4509–4531.
- Shepherd, T.G., J.N. Koshy, and K. Ngan, 2000: On the nature of large-scale mixing in the stratosphere and mesosphere. *J. Geophys. Res.*, **105**, 12433–12446.
- SPARC, 2002: SPARC Intercomparison of Middle Atmosphere Climatologies. SPARC Report No. 3 (ed. W. Randel, M.-L. Chanin and C. Michaut), WCRP-116, WMO/TD No. 1142.
- Sparling, L.C., 2000: Statistical perspectives on stratospheric transport. *Rev. Geophys.*, **38**, 417–436.
- Sparling, L.C., J.A. Kettleborough, P.H. Haynes, M.E. McIntyre, J.E. Rosenfeld, M.R. Schoeberl, and P.A. Newman, 1997: Diabatic cross-isentropic dispersion in the lower stratosphere. *J. Geophys. Res.*, **102**, 25817–25829.
- Strahan, S.E. and J.D. Mahlman, 1994: Evaluation of the SKYHI General Circulation Model using aircraft N₂O measurements. 2. Tracer variability and diabatic meridional circulation. *J. Geophys. Res.*, **99**, 10319–10332.
- Tegtmeier, S. and T.G. Shepherd, 2007: Persistence and photochemical decay of springtime total ozone anomalies in the Canadian Middle Atmosphere Model. *Atmos. Chem. Phys.*, **7**, 485–493.
- Thuburn, J. and G.C. Craig, 2002: On the temperature structure of the tropical stratosphere. *J. Geophys. Res.*, **107**, 4017, doi: 10.1029/2001JD000448.
- Trepte, C.R. and M.H. Hitchman, 1992: Tropical stratospheric circulation deduced from satellite aerosol data. *Nature*, **355**, 626–628.
- Volk, C.M., J.W. Elkins, D.W. Fahey, R.J. Salawitch, G.S. Dutton, J.M. Gilligan, M.H. Proffitt, M. Loewenstein, J.R. Podolske, K. Minschwaner, J.J. Margitan, and K.R. Chan, 1996: Quantifying transport between the tropical and mid-latitude lower stratosphere. *Science*, **272**, 1763–1768.
- Walker, K.A., C.E. Randall, C.R. Trepte, C.D. Boone, and P.F. Bernath, 2005: Initial validation comparisons for the Atmospheric Chemistry Experiment (ACE-FTS). *Geophys. Res. Lett.*, **32**, doi: 10.1029/2005GL022388.
- Waugh, D.W., R.A. Plumb, R.J. Atkinson, M.R. Schoeberl, L.R. Lait, P.A. Newman, M. Loewenstein, D.W. Toohey, L.M. Avallone, C.R. Webster, and R.D. May, 1994: Transport out of the lower stratospheric Arctic vortex by Rossby-wave breaking. *J. Geophys. Res.*, **99**, 1071–1088.
- Waugh, D.W. and T.M. Hall, 2002: Age of stratospheric air: Theory, observations, and models. *Rev. Geophys.*, **40**, 1010.
- Williamson, D.L. and P.J. Rasch, 1989: Two-dimensional semi-Lagrangian transport with shape-preserving interpolation. *Mon. Wea. Rev.*, **117**, 102–129.
- Yulaeva, E., J.R. Holton, and J.M. Wallace, 1994: On the cause of the annual cycle in tropical lower stratospheric temperatures. *J. Atmos. Sci.*, **51**, 169–174.